UNIVERSITY OF CALIFORNIA SAN DIEGO

Small autonomous landers for studying the community ecology of nearshore submarine canyons

A thesis submitted in partial satisfaction of the requirements for

the degree Master of Science

in

Marine Biology

by

Ashley M. Nicoll

Committee in charge:

        Phil Hastings, Chair
        Anela Choy
        Natalya Gallo
        Brice Semmens

2021

The thesis of Ashley M. Nicoll is approved, and it is acceptable in quality and form for publication on microfilm and electronically.

University of California San Diego

2021

Table of Contents

List of Tables

List of Figures

Acknowledgements

This thesis would not have been possible without the help of many individuals along the way. I would like to thank my committee chair, Phil Hastings, who took me on during my undergraduate degree to work in the Marine Vertebrate Collection and then was willing to help me continue to explore my interest in fishes and ecology through a master's degree.

Natalya Gallo, my mentor throughout the entire master's process. She dedicated many hours to teaching me how to be a better and more inquisitive scientist. I am very appreciative of the time invested in my success as a student even while Natalya moved across the world to Norway. I really appreciate her quick feedback on all my work including manuscripts, conference materials, and presentations.

I would also like to thank and acknowledge my other committee members who gave me excellent feedback and opportunities throughout the master's program. Thank you to Brice Semmens for your thought provoking questions and great feedback. Thank you to Anela Choy for your assistance in data processing from video as well as the opportunity to go to sea for a research cruise. My committee was extremely supportive throughout the entire master's process, especially through the pandemic.

This entire project would not have been possible without the gracious help of Kevin Hardy. Natalya introduced me to Kevin Hardy early in the master's program, with the promise that it would be a quick retrofit of *DOV BEEBE* with a new camera system and we'd be back in the water. Many lunches, a new lander, and an entirely new camera and lights system later Kevin had us back in the water. I would not have traded all the hours spent in Kevin's shop for anything, I am extremely grateful for his patience in teaching me all about engineering and his

viii

ABSTRACT OF THESIS

Small autonomous landers for studying the community ecology of nearshore submarine canyons

by

Ashley M. Nicoll

Master of Science in Marine Biology

University of California San Diego, 2021

Professor Phil Hastings, Chair

Nearshore submarine canyons are unique features that bring the deep sea close to shore, potentially functioning as highways connecting shallow and deep-sea ecosystems. To study their ecology, we developed two autonomous lander systems: a 2-sphere Picolander for exploratory deployments (< 3 days) and a 3-sphere Nanolander for longer deployments (> 1 week). Both landers were outfitted with a camera and lights system and a ZebraTech environmental sensor and collected paired physical and biological time series. Eleven lander deployments were

completed ranging in length from 1-13 days at depths of 90-500 m, allowing assessment of how seafloor community diversity and composition changed with depth and time of day. We found that communities at 100 and 500 m were distinct from all other depths while the 300 m community was transitional between these depths and had the highest diversity, despite unexpectedly high turbidity. Additionally, we recorded clear diurnal patterns in fishes deeper than 300 m, as well as vertical migration of larval flatfish. This study also aimed to document the number and area of small submarine canyons off the coast of California and determine the extent of government protection of both large and small canyons. Small canyons were defined as features with a minimum depth of 200 m and incised 100 m into the slope. Applying this, 23 small canyons were identified, with features concentrated on the Central and Southern coast. By area, 27% of large canyons and 23% of small canyons were protected, with the inshore reaches of canyons receiving more protection than offshore. Because landers collect paired biological and physical data in hard to access areas, they may serve as powerful tools to inform management of these poorly studied deep-water habitats.

Introduction

  Submarine canyons throughout the US Exclusive Economic Zone (EEZ) and beyond are

typically understudied because they are difficult areas to access due to their extreme depths and

proximity to shore. Shepard (1963) defined submarine canyons as "steep-walled, sinuous valleys

with V-shaped cross sections, axes sloping outwards as continuously as river-cut land canyons

and relief comparable to even the largest of land canyons."   Despite being understudied, these

are not rare ecosystems. Fernandez-Arcaya et al. (2017) identified over 9000 large canyons that

cover approximately 11.2% of continental slopes globally. On the Pacific coast of North

America, submarine canyons cut over 20% of the continental shelf with that cover approaching

50% at latitudes north of 45 degrees (Kunze, 2002).

Ecological Attributes of Submarine Canyons

  Both nearshore and offshore submarine canyons are "keystone structures" for local

marine communities that provide ecosystem services to the surrounding area (De Leo, 2017).

Ecosystem services are divided into three categories: supporting services, regulating services,

and provisioning services (Fernandez-Arcaya et al, 2017). Supporting ecosystem services are

defined as those that have an indirect effect on human well-being. Canyons serve this purpose by

supporting the transfer of nutrients from the shelf to the deep sea. This transfer of nutrients

provides an increase in food resources and allows canyons to be nurseries as well as refuge

grounds. Regulating services are the benefits of the natural buffering functions of the canyons.

Canyons provide this through high particulate transport and increased carbon cycling, regulating

carbon storage and burial of waste such as pollutants. Provisioning services refer to the products

directly obtained from the ecosystem such as the fish or other organisms living in the canyons.

It has been proposed that submarine canyons concentrate motile megafauna such as fishes, known as the "canyon effect" (De Leo, 2010). The comparison has been made that canyons are to demersal species as upwelling locations are to pelagic species (Company et al., 2008). This phenomenon, known as the canyon effect, has been documented by several other studies in various parts of the world. Additionally, it has been shown that the La Jolla Canyon may have as much as 50 times the macrofaunal biomass than the surrounding areas of the shelf and slope (Vetter & Dayton, 1998). It is important to characterize the seafloor communities present in these unique bathymetric features to properly inform policy aimed at protecting these areas.

Biogeochemical Attributes of Submarine Canyons

Nearshore submarine canyons are unique bathymetric features that bring the deep sea close to shore, potentially functioning as "highways" between shallow and deep-sea ecosystems. Evidence of the highway function can be seen in the Scripps and La Jolla Canyons through the littoral cell, a coastal compartment that contains a complete cycle of sedimentation including sources, transport paths, and sinks (Inman, 2005), that intersects the heads of both canyons (Brueggeman, 2009). This littoral cell carries materials such as plant matter and garbage from Dana Point south into the canyons. Rapidly moving currents transport and deposit materials down the canyons into the deep ocean. The transport of coastal materials (i.e., plant matter) is a function unique to nearshore canyons.

Oxygen in Submarine Canyons

Submarine canyons are known to be areas of localized upwelling. The current in a canyon typically aligns with the canyon axis which can result in local upwelling bringing

nutrients into the euphotic zone and promoting primary production (Ryan et al., 2005). In seasons with strong thermohaline stratification, the flow of water in the upper water column may decouple from the deep water. This results in the deep water continuing to follow the canyon axis while the upper water column follows its original path. This type of current flow can induce and focus internal waves (Hall & Carter, 2011; Fernandez-Arcaya et al., 2017). Internal waves have been proposed as the main driver of environmental variability within canyons including contributing to elevated turbulence in these areas (Hamann, 2019).

Oxygen conditions in submarine canyons tend to approximate local oxygen gradients. In eastern boundary upwelling regions or areas with oxygen minimum zones, such as off San Diego, severely hypoxic conditions are possible. Nanolander deployments conducted in 2016 off the coast of Del Mar, just north of the La Jolla Canyon, can provide some additional details on the oxygen variability potentially experienced in the canyon on shorter timescales. These deployments found that hypoxic conditions occurred at depths of ~200 m, ~300 m, and ~400 m (Gallo et al., 2020). At ~200 m hypoxic conditions only occurred for relatively short portions of the deployments, hypoxic conditions were recorded for ~13% of a 15-day fall deployment to ~200 m (Gall et al., 2020). At depths of ~300 m and ~400 m, oxygen conditions were continuously hypoxic, and at ~400 m they were severely hypoxic (i.e., $O_2 < 22.5$ µmol kg^{-1}) (Gallo et al., 2020). While hypoxic conditions were never experienced at ~100 m, the difference in mean oxygen conditions between ~200 m and ~100 m was quite small (Gallo et al., 2020).

Environmental data collected from a nearby CalCOFI station (93.3. 28) can provide additional context for variability potentially experienced in the La Jolla Canyon on longer timescales. When examining quarterly CalCOFI profiles from the past ~16 years, we can see that temperature variability is highest in the upper water column (< 50 m) and is relatively low deeper

than 150 m. In contrast, the absolute oxygen variability (standard deviation) is highest between 50 and 150 m and the coefficient of variation (CV) for oxygen increases below 100 m (Gallo et al., 2020).

Submarine Canyon Definitions

Traditionally, large offshore submarine canyons as defined by Harris and Whiteway (2011), "which requires canyons to extend over a depth range of at least 1000 m and to be incised at least 100 m into the slope at some point along their thalweg," have been at the forefront of submarine canyon research. However, neither of the definitions presented in this paper thus far include nearshore submarine canyons and consequently they have been neglected and their importance to both physical and biological processes in nearshore environments is poorly studied. This is especially true for smaller scale canyons that come in close to the shore such as the La Jolla Canyon that are too small to be captured by the characteristics described above.

Submarine Canyon Protection

Of the approximately 9,000 submarine canyons worldwide, only about 22% are protected by Marine Protected Areas (MPA) (Fernandez-Arcaya et al, 2017). Additionally, 83% of countries have less than 10% of their large submarine canyons inside an MPA (Fernandez-Arcaya et al., 2017). The United States has about 117 large submarine canyons within its EEZ, 43 of those are in California. However, most of the conservation policy in US waters is focused on the shelf rather than the slope (Fernandez-Arcaya et al., 2017). It is unlikely, however, that these protection numbers account for the smaller nearshore submarine canyons as they are hard to reach and often outside of the parameters used for global-level bathymetric studies. Thus, the

specifics of this definition may result in the smaller canyons receiving less scientific and management attention.

Methodology to Study Submarine Canyons

Nearshore submarine canyons tend to be understudied ecosystems because they are hard areas to reach due to their proximity to land and narrow structure. Traditional deep-sea study mechanisms include underwater vehicles, towed cameras on sleds, and trawls. These study tools typically require a medium or a large vessel equipped with a winch and A-frame as well as the capacity to accommodate hundreds of meters of cable on deck. The usage of such vessels is costly, time consuming, and logistically complicated when close to shore. The biology of the deep-sea is traditionally studied using trawls, which often pose its own challenges. Because canyons are constricted areas with significant relief, trawls are destructive and may get caught up in these areas. In order to avoid challenges associated with trawling complex underwater structures, autonomous lander systems can be used to collect environmental and biological data from small nearshore submarine canyons and greatly reduce the costs and impacts associated with studying near-shore, deep-sea ecosystems.

A Brief History of Lander Technology

The usage of landers for studying the deep-sea benthos has a long history with the first proposed usage in 1938 (Ewing & Vine, 1938). Landers are autonomous, positively buoyant modular vehicles with either an on-board timer or acoustic release which causes it to drop its ballast and float back to the surface. Landers were initially explored as an alternative to cabled observations from large research ships to decrease the cost and increase the deployment lengths associated with deep-sea observations (Ewing and Vine, 1938). The first autonomous lander

system was developed with seismic equipment installed. After the first autonomous landers were successfully used, their popularity and applications grew rapidly including photographing and collecting bottom creatures for biochemical studies, measuring bottom currents, sampling bottom water, recording deep-sea tides and temperatures, and collecting sediment samples (Phleger & Soutar, 1971).

Early landers were constructed in a linear fashion on long cables that required large vessels with a lot of deck space to accommodate. Additionally, each element on the cable was lowered into the water using a winch on the vessel. In the late 1990's and early 2000's lander technology started to evolve to become smaller easing transport and operation (Priede and Bagley, 2000). Most studies that used benthic landers examined biogeochemical fluxes with a large focus on sediments and pore water. Since 1960, landers were frequently outfitted with a pyramid shaped trap to facilitate the collection of benthic animals to study demersal fishes and other deep-sea organisms (Isaacs, 1960). The first lander equipped with a camera capable of photographing deep-sea animals was also developed in 1968 (Sessions et al., 1968). The integration of camera systems allowed biologists to study animals that cannot be captured and recovered in traps on the landers. As camera technology evolved, the cameras used on benthic landers improved as well.

The first landers designed to be deployed to the hadal zone (> 6500 m) to study biology at extreme depths diverged from the linear design of the original landers to a more compact design with a metal frame for attachment of scientific equipment (Jamieson, 2009). These landers were still heavy and quite large. Despite necessitating a large vessel for transport, advances in lander technology have greatly increased the ease of deployment by reducing the risk of tangling of cabled instruments.

While the design of having a large metal frame to attach the scientific payload remains quite common for deployable equipment, two modified lander designs have become popular for biological studies. The first design is a large box-shaped lander (Peoples et al., 2019). The box shape is a robust design that allows the lander to be rated for full-ocean-depth and to carry a diverse scientific payload. Similar to their metal frame counterparts, box landers are large and heavy, requiring a winch to deploy them off the side of a large research vessel. The second lander design aims at making the lander as small as possible to decrease the cost of deep-sea research by reducing the reliance on large vessels. These landers are vertically oriented and use spheres for instrument housings as well as flotation (Gallo et al., 2020; T. Miwa, 2016). Their primary usage is ecosystem monitoring. The landers used in this study fall into this design category and will be discussed further.

Landers for ecosystem monitoring have trended toward becoming smaller in size with high-resolution time-lapse cameras, LED light systems, and environmental monitoring tools such as a CTD/DO sensor. The landers used in this study, Nanolander *DOV BEEBE* and Picolanders *DOV JEAN* and *DOV LEVIN*, follow this trend. A remarkably similar lander to the ones developed for this study, was developed for ecosystem monitoring in Japan (T. Miwa, 2016). The lander, named "Edokko no.1", is equipped with a camera system, LED lights, as well as a CTD/DO sensor. It uses three-spherical glass housings to hold the camera, batteries, and communication system. All the spheres are set inside of a rubber frame in a vertical orientation. The lander was constructed to be small so that it can be deployed and recovered from a small fishing vessel to a depth of up to 10,000m. "Edokko no. 1" weighs between 50 and 60 kg in air and is deployed with 40 kg of sacrificial weights (T. Miwa, 2016). The overall design of "Edokko no. 1" is very similar to *DOV BEEBE* (Gallo et al., 2020). *DOV BEEBE* incorporates

three-spherical housings for equipment and a CTD/DO sensor. The primary difference between

the Japanese lander and the one used in this study are the materials used to construct the frame as

well as the spherical housings. The frame for *DOV BEEBE* is made from marine-grade high-

density polyethylene (HDPE) (brand name "Starboard") and the spheres are made of injection-

molded polyamide with 30% glass fibers for increased strength. Both materials are lightweight in

and out of water which results in a large weight reduction between the two lander designs. In air,

DOV BEEBE weighs approximately half of what "Edokko no. 1" is reported to weigh and can be

deployed with half the sacrificial weights. However, by using glass spheres "Edokko no. 1" is

capable of being deployed to deeper depths than *DOV BEEBE*, which is equipped with the

injection molded polyamide and glass spheres. While it is possible for *DOV BEEBE* to be

outfitted with glass spheres for housing, for the purpose of this study the polyamide spheres

provided increased durability and ease of use compared to glass.

The lander framework used in this study has two parts: the Picolander *DOV JEAN* and

Nanolander *DOV BEEBE*. Both landers were designed and built (Global Ocean Design LLC, San

Diego, CA) with the goal of reducing the costs associated with studying deep-sea ecosystems

and therefore, increasing accessibility to information about these unique areas.

The La Jolla Canyon

This study aims to use the La Jolla Canyon as a testbed for the lander framework as a tool

to study nearshore submarine canyons. Previous research into the community ecology of this

canyon is limited. More than 2/3 of papers published on the Scripps and La Jolla submarine

canyons before 2010 were published in journals of geology, geophysics, and sedimentology

(Brueggeman, 2009). Papers published in journals of ecology accounted for only 5% of papers

listed in Brueggeman's Canyon Bibliography. The prior research on community ecology in the

canyons was primarily done via submersibles. However, in one study, over half of the video data were unusable due to obscured camera footage (Vetter, 1999). Despite the sampling issues experienced by the researchers, they found evidence that plant debris aggregates supported a large amount of benthic production in the canyons. The researchers also found evidence that fish abundances were enhanced inside the canyon when compared to the nearby upper margin (Vetter, 1999).

Objectives of this study include the following.

Objective 1: How do landers perform as tools to study nearshore submarine canyons?

Hypothesis 1: The landers will perform well in collecting environmental and biological data in nearshore submarine canyons.

Objective 2: How does seafloor community diversity and composition within the canyon change with depth?

Hypothesis 2: The seafloor community composition will differ across depths and will decrease in diversity deeper in the canyon. We expect this decrease in diversity to be due to lower mean oxygen conditions at deeper depths as well as a decrease in diurnal community changes.

Objective 3: What are the effects of day and night on the seafloor community composition within the La Jolla Canyon? Is this effect impacted by depth?

Hypothesis 3: The seafloor community composition will exhibit differences between day and night, due to certain species having nocturnal versus diurnal preferences. We expect day/night differences to lessen with increasing depth, where less sunlight penetrates.

Objective 4: Documentation of the number and area of small submarine canyons off the coast of California and determination of the extent of government protection of both large and small canyons.

Hypothesis 4: Small, nearshore submarine canyons have less area protected than their larger submarine canyon counterparts.

Methods

<u>Lander Framework</u>

To better understand the ecology of nearshore submarine canyons, two low-cost, spatially flexible autonomous lander systems were used: the Nanolander *Deep Ocean Vehicle (DOV) BEEBE* and Picolander *DOV LEVIN* (Fig. 1). Both landers were designed and built (Global Ocean Design LLC, San Diego, CA) with the goal of reducing the costs associated with studying deep-sea ecosystems and therefore, increase accessibility to information about these unique areas. The Nanolander has three spherical housings containing a camera system, an acoustic communication system, as well as a Zebra-Tech Moana sensor for measuring temperature and depth. The smaller, two-sphere Picolander is equipped with a Zebra-Tech sensor, camera system, and timed release for 24-hour deployments. Both systems are positively buoyant and deployed by hand from a small boat (Fig. 1). The Nanolander system can collect paired biological and physical data in the deep sea over a greater timescale (i.e., several weeks) than traditional methods (e.g., several hours, if using a submersible). The landers are almost fully rechargeable between deployments, requiring only the sacrificial weights be discarded to terminate each deployment.

The Nanolander, *DOV BEEBE*, was developed by Kevin Hardy and Natalya Gallo (Gallo et al., 2020; Global Ocean Designs LLC) in 2016. The Picolander, *DOV LEVIN,* was developed to be a modular attachment to a larger lander design and made into a stand-alone lander by Kevin Hardy and Mare Sutphen. The camera and lights systems of both landers were developed by Kevin Hardy and Ashley Nicoll. *DOV BEEBE* stands at 1.6 m tall and 0.86 m wide while *DOV LEVIN* stands at 0.64 m tall and 0.86 m wide (Fig. 1). When deployed, the Nanolander floats ~0.5 m from the ocean floor and the Picolander about 1 m, allowing the camera port to be at

approximately the same height for both landers (Fig. 3d). This distance is determined by the length of the anchor chain connecting the lander to its weights. At this height, the horizontal field of view is approximately seven m by three m in ideal visibility conditions. This was determined by diving on the lander while it was recording and swimming out with a meter tape. The frames of the landers are built from marine-grade high density polyethylene (HDPE) from the brand Starboard and reinforced with fiberglass. HDPE has a specific gravity of <1 and the specific gravity of fiberglass is ⅔ that of aluminum, requiring little flotation for the lander to reach neutral buoyancy. The frame is held together with 316 stainless steel fasteners.

Within the lander frames are glass-filled polyamide spheres with diameters of 25.4 cm. These spheres are utilized as both instrument housings as well as floatation allowing the vehicles to be smaller and lighter than previous generations of landers. Glass spheres have the advantage of deeper operational depths (~11 km), the glass-filled polyamide spheres were chosen due to machining advantages and decreased costs. The spheres used for the landers are pressure tolerant to 2 km depth. Attached to the frames of both landers is the Zebra-Tech Moana TD1000 temperature and depth sensor. The Moana is a fully autonomous instrument that was developed as part of the Moana Project (moanaproject.org). Initial sensor accuracy +/- 0.05 °C for temperature and +/- 0.5% for pressure measurements. The Moana TD1000 is rated to 1000 m with a memory capacity of 62,284 records (1 record = depth, temperature, time, and date).

The Nanolander hosts three spheres, the top sphere holds an Edgetech BART (Burn Wire Acoustic Release Transponder) board, which is used to communicate with the Nanolander while it is deployed. A transducer is bonded to the outside of the top sphere and positioned within the lander frame to point upwards. The EdgeTech BART board has four programmable commands that are used to enable and disable communications and initiate the burn for recovery. An

overboard transducer and EdgeTech deck box are used to communicate with the lander from the boat. The battery for the BART board and for the burn wires is also housed in the upper sphere. After the release command was sent, the burnwires take ~6.5 min to burn and then the Nanolander ascends through the water column at a rate of ~60 m min^{-1}. Upon arriving at the surface, the Nanolander floats vertically due to inherent stability in the design where the weight is placed low, and buoyancy is placed high (Fig. 1, Fig.2b). This feature makes visual detection of the lander easy in good conditions due to the brightly colored spheres and the flag (Fig. 3b). Additionally, floating vertically allows the GPS system (Spot Trace), positioned at the top of the frame, to connect to satellites upon arrival to the surface. The middle sphere functions as the "battery pod" and hosts two 16 Ah (ampere hour) lithium polymer (LiPo) batteries (Multistar) and individual battery management systems with a low voltage cutout (LVCO) for each battery. The battery pod is used to power the two-external light-emitting diode (LED) lights. The LiPo batteries are charged via an external port so that the sphere does not have to be opened. The bottom sphere houses the camera system and timelapse relay both of which are newly developed and shared with the Picolander, discussed in detail below.

The Picolander hosts two spheres. Like the Nanolander, the Picolander's upper sphere hosts the elements required for the release, however, the Picolander uses a timed-release system. The upper sphere of the Picolander has two timers, with maximum times of 99 hours, each with their own nickel-metal hydride (NiOH) (Tenergy) rechargeable batteries. The two timer and NiOH battery systems are each attached to one of the two burn wires mounted on the bottom of the lander. The timers themselves are powered with 1.5 V (volt) LR-44 batteries and the NiOH batteries serve to provide the voltage that runs through the burn wires to initiate the release. Setting the two timers approximately 30 minutes apart provides a redundant release mechanism.

After the timer goes off, the burnwire takes approximately 10-15 minutes to burn. Then the Picolander ascends through the water column at a similar rate to the Nanolander ($\sim$60 m min^{-1}). Also housed in the first sphere is a Spot Trace GPS. The Spot Trace is mounted in the upper hemisphere of the top sphere so that it is out of the water upon recovery and can start broadcasting its location when the lander surfaces.

The camera is housed in the bottom sphere of both landers. As stated above, this camera sphere was newly designed for this project and is the same in both landers. In addition to the camera, this sphere houses a time-lapse controller, V50 Voltaic battery pack to power the camera, a 16 Ah LiPO battery for powering the LEDs, and the LED drivers (Fig. 2a, c). The sphere itself has a "port hole" where the camera looks out that is made of 1-inch-thick acrylic. The camera is a GoPro Hero 4 and is controlled by a CamDO Blink time-lapse controller. The time-lapse controller is programmed via Wi-Fi to set the interval and the action for the camera. This Voltaic brand battery pack was selected specifically because it has no low-power auto-off function and was recommended by the company CamDO. When the CamDO turns on the GoPro, a small amount of that voltage is run through a mosfet to the LED drivers. This turns on the LED lights powered by the LiPO battery. By using this method, the system is completely powered off between recording intervals allowing the battery power to be conserved. This is an improved camera sphere design from that previously used in Gallo et al. (2020), which had a small continuous power draw. In the Picolander, the one 16 Ah LiPO battery in the camera sphere is used to power the lights. In the Nanolander, the camera sphere and battery pod have an additional connection that allows all the LiPOs to be in parallel permitting the use of all 48 Ah of LiPO batteries on board for powering the LED lights.

To understand how much data could be collected with the novel Picolander and new camera system, a bench test of the battery capacity was conducted. All the batteries were charged fully and then set to record for the planned deployment intervals, 20 seconds of video every 20 minutes. The lander was left on the bench to run both the camera and the lights until the batteries ran out. The video clips were then used to evaluate maximum duration of battery power. This test was conducted with the V50 Voltaic Systems battery pack powering the GoPro and CamDO and a 16 Ah LiPO battery powering the LED lights.

DOV BEEBE is equipped with a drop arm on the front side. The drop arm is secured during deployment using three "Wint-O-Green" Lifesavers. The drop arm was used to hold bait for each Nanolander deployment, and it also had a ~15 cm cross bar for size reference. The bait for every deployment except for one was 2 frozen pacific chub mackerel (*Scomber japonicus*) and was secured to the drop arm using dissolvable thread. The deepest deployment used assorted frozen demersal fishes collected from the area. All bait was consumed on each deployment. Only the Nanolander deployments were conducted with bait because the Picolander did not have an attached drop arm or crossbar.

Both landers are positively buoyant in water and are deployed with sacrificial weights. The Nanolander is deployed with ~20 kg (45 lbs) of weight while the Picolander is deployed with ~ 11 kg (25 lbs). The weights are attached by a sliding link on a metal chain. The metal chain is secured on each side of the landers using a burn wire. The release of either burn wire will allow the metal chain to slide through the link and the lander will float back to the surface. The estimated descent rate of the landers is ~100 m min^{-1}, and the ascent rate ~ 60m min^{-1}. Once on the surface the landers float ~0.45 m out of the water and have brightly colored flags to aid in

visual detection (Fig 3b, c). The Nanolander is deployed with one additional flotation sphere to increase the buoyancy.

Six successful exploratory deployments were conducted with the Picolander (Fig. 5). These deployments ranged in length from 26 to 51 hours and targeted depths from 100 to 500 m (Table 2). The goal of these deployments was to preview sites for longer Nanolander deployments. For all deployments, the camera was set to record video for 20 seconds every 20 minutes.

Five successful deployments of eight to 12 days were conducted with *DOV BEEBE*. *DOV BEEBE* re-occupied deployments sites from the Picolander except for one site, Pico-D370 (Table 1, Fig. 5).

Characterizing Environmental Variability

Environmental data are collected by the Zebra-Tech Moana temperature and depth sensor that is connected to the frame of both the Picolander and the Nanolander. The Moana is a fully autonomous instrument. While in air, the Moana processes atmospheric pressure measurements to maintain a baseline of sea level ambient pressure. A change in pressure relative to the baseline triggers the start of a dive. During a dive, the Moana records the depth and temperature every second while the pressure is changing, and a sample is taken every 5 minutes when the depth is constant. Constant depth is defined as a change of less than 1 m when in 200 m or less water or by more than 4 m at a depth of more than 200 m. Additionally, the Moana will not record data for a depth it has already recorded during the previous 30 seconds, this filter limits repetition in the data in conditions such as during shallow deployments with high wave activity. When the sensor is in contact with air following a dive, it broadcasts a Bluetooth signal allowing the data

from the sensor to be offloaded using the Zebra-Tech BLE application for IOS. The data are offloaded as a comma-delimited file for easy sharing to other devices.

For each deployment, a time series of depth over time colored for temperature was constructed to get a visual representation of the range of conditions over the deployment. The mean and ranges of conditions were compared across the deployments and depths. Data from both the Picolander and the Nanolander deployments were included (Table 1, Table 2).

Characterizing Differences in Seafloor Community and Diversity

The GoPro Hero 4 camera was programmed to record 20 seconds of video every 20 minutes throughout the deployment. After a deployment was conducted, the SIM card from the GoPro was removed and the files were offloaded to a computer. In this study all video clips were annotated and vertebrate species within the frame were identified to the lowest taxonomic level and counted. Invertebrates were also noted and counted. Because visibility has an effect on how well organisms can be identified and counted, each clip was categorized by visibility quality using the following categories: A (seafloor is visible, water column is rather clear, very good quality), A- (seafloor is visible, water column has some turbidity, good quality), B (cannot make out the sediment type, water column is quite turbid, poor quality), B- (only the drop arm is visible, the water column is very turbid, very poor quality), and C (the drop arm is not visible, no visibility). Only samples with visibility A or A- were used for subsequent community analyses.

The methods for assessing community-level differences across deployments were based on the methods from Gallo et al. (2020) and used non-metric multidimensional scaling (nMDS) with the "vegan" package in R (Oksanen et al., 2017). The nMDS analyses used a Wisconsin double standardization and the counts were transformed with a square-root transformation. These are used with data that have a high range of counts and have been shown to improve the nMDS

17

results (Oksanen et al., 2017). Bray–Curtis dissimilarity was used as the input, and community dissimilarities were mapped onto ordination space for the nMDS analysis. Prior to running the nMDS, all video samples with no organisms observed were removed and only clips with visibility A or A- were used for analysis. Additionally, rare operational taxonomic units (OTUs) (OTUs observed less than 8 times) were removed from the matrix. This resulted in 1564 video clips with 29 unique OTUs for analysis. The environmental data were paired with the video samples using the timestamps from both the Moana TD1000 and the GoPro Hero 4. Because the Moana TD1000 takes a sample every 5 minutes, about every 4th value was used to match with the video sampling intervals (i.e., 20 seconds of video every 20 minutes).

To examine differences in community diversity between deployments, species accumulation curves plotted against the number of video samples were used. Species accumulation curves were selected because the number of video samples differed between deployments (Hurlbert, 1971; Simberloff, 1972; Heck et al., 1975). The community matrix used in the nMDS plots was modified to show presence / absence of OTUs rather than counts of OTUs observed in each sample. A function was written in R that loops through the community matrix to construct a rarefaction curve for each unique deployment. In this matrix, each column represents a different OTU. The code runs through each unique deployment, each of which contains a number of samples "n." For each deployment, the script pulls a number of random video clips "i" from 1 to n. For each value of i, each column is summed. If the column has a value of zero, the zero is kept. Otherwise, the value is replaced with a 1. In this way, we create a logical index of OTUs presence. This process is repeated 100 times for each deployment. The data are stored in a data frame with the deployment number, number of samples pulled, and the number of unique OTU observed. The data are aggregated to find the mean number of unique

18

OTUs observed each time i samples are pulled. This creates a new data frame with the mean number of unique OTUs observed per i samples in each unique deployment. The aggregated mean number of unique OTUs per i samples in each deployment is plotted using the package "ggplot2". Species accumulation curves were constructed for Picolander and Nanolander deployments. For Nanolander deployments, species accumulation curves were made using both samples with only visibility category A or A- as well as with all samples. This was done because the 300 m deployment had poor visibility for much of the deployment and the species accumulation curve did not level off when using only samples with A or A- visibility.

Characterizing Differences in Demersal Fish Community and Diversity

The demersal fish community was analyzed using the species balance, Berger-Parker index of dominance (Berger & Parker, 1970), and species richness. Demersal fishes were selected because some deployments had consistently high numbers of sessile invertebrates that did not move over the duration of the deployment and some deployments had extremely high numbers of anchovy (*Engraulis mordax*) schools that could introduce bias. The distribution of demersal fishes present was also analyzed using violin plots. The demersal fish community composition was analyzed using video samples with visibility A or A- only and samples with no observations were excluded. The R package "diverse" (Guevara, 2017) was used to calculate the species balance. The species balance was calculated as a proportion and plotted using a stacked barplot. The same samples used for the species balance were also used to calculate the Berger-Parker index of dominance. The index was calculated for each video sample in a deployment and then used to find the mean and standard deviation over the course of the deployment. The inverse value was also calculated so that an increase in the value of the index represents an increase in diversity and a reduction in dominance. The number of demersal fish per video clip by

deployment was plotted using violin plots. Only samples with A or A- visibility and with demersal fish observed were used. Demersal fish were present in 53% of Nanolander samples with visibility A or A- and in 44% of Picolander samples.

Diurnal Patterns

Daily patterns of when common species were recorded were also examined. This was done by plotting all observations and abundances of a species across all deployments where they were observed against time of day on the x-axis. For this analysis sunrise is defined as 0600 and sunset is defined as 1800 to be consistent across all deployments. The commonly observed species used for this analysis were: Dogface Witch Eels (*Facciolella equatorialis*), Blackmouth Eelpouts (*Lycodapus fierasfer*), Black Eelpouts (*Lycodes diapterus*), Halfbanded Rockfish (*Sebastes semicinctus*), larval flatfish, and anchovies (*Engraulis mordax*).

To assess changes in the community over the course of a single deployment, nMDS analyses were performed to look at differences in communities in relation to the environmental variables collected over the course of the deployments (temperature, depth, and time of day). To examine communities with respect to diurnal cycles, the video samples from the deployments were grouped into day and night categories according to the times for sunrise and sunset during the deployment period. Only Nanolander samples with visibility categories A or A- were used for analysis and samples with no organisms present were removed. Additionally, rare species (< three observations over the course of Picolander and Nanolander deployments) were omitted from the community matrices. The resulting number of video samples and species incorporated into the analyses for each deployment are summarized in tables 1 and 2.

Comparing Lander Results to Records in the Marine Vertebrate Collection at SIO

A comparison between local, canyon associated species in the Scripps Institution of Oceanography (SIO) Marine Vertebrate Collection (MVC) and the fish species observed by both the Pico-and the Nanolander was conducted to investigate how many species were common between the two datasets, and how many were unique. This analysis was done with data from Hastings et al. (2014). This paper summarized the fishes of La Jolla and the local Marine Protected Areas based on records of specimens in the MVC. Collection of specimens in the MVC began in 1905 and continues to the present day. Specimens from La Jolla that were collected at the La Jolla or Scripps canyons at a depth greater than 30 m were annotated with "Canyon" by Hastings et al. (2014). Because the study area for the landers began at 100 m, fish whose depth range are shallower than 100 m were filtered out. Depth range limits were determined with Miller and Lea (2020). The modified species list from Hastings et al. (2014) is summarized in supplementary Table 1. This list was then compared to the fish species observed throughout all lander deployments. This was done to test the efficacy of these lander deployments in characterizing fish community diversity in the La Jolla Canyon system, compared to many years of collections.

Identifying Small Submarine Canyons

To determine the amount of protection afforded US West Coast small, nearshore submarine canyons, we first had to determine how many were present. Methods for identifying small submarine canyons on the coast of California were adapted from the methods from Harris et al. (2014) using Arc-GIS Pro. We used 1-arc second resolution bathymetry from the National Oceanic and Atmospheric Administration (NOAA) Coastal Relief Model – Southern California Version 2, for the California coast from the border with Mexico north to Monterey Bay (Fig. 4a).

North of Monterey Bay, only 3-arc second resolution bathymetry was available. We found that 3-arc second resolution is not sufficient for identifying small submarine canyons. Additionally, North of Monterey Bay the shelf widens and bathymetric features tend to be larger and further offshore. We used a topographic position index (TPI) to examine the ruggedness of the bathymetry (Fig. 4b). TPI was evaluated using 10, 5, and 3 cell radii, and the cells with values over 5 in these TPI layers were extracted and converted into vector polygons. These layers were merged and used in conjunction with 10- and 100-meter contours to help identify locations for small submarine canyons. After potential locations were identified, we checked them against our previously stated definition of extending to a minimum depth of 200 m and incised into the slope at least 100 m. The canyons that fit this definition were then manually digitized (all features were digitized at a 1:150,000 scale) and grouped into one of three categories: nearshore (within five km of coastline), offshore (> five km from coastline), and extension of a large canyon (a section of a larger canyon from Harris et al., 2014). Extensions of large canyon systems included both nearshore and offshore canyon features. Once the canyons were digitized, they were smoothed and buffered out by 1 arc-second to account for the resolution of the bathymetry (Fig. 4c).

Protected Areas of Submarine Canyons off the Coast of California

After all canyons were digitized, their area overlap with protected areas was evaluated using the intersect tool in ArcGIS Pro. Prior to calculating the intersect, all layers were projected to NAD83 (meters) to ensure the correct units. The protection of the canyons was evaluated by calculating the intersection between the large and small canyons and the following protected areas: Marine Protected Areas (MPAs), National Marine Sanctuaries (NMSs), and Cowcod Conservation Areas (CCAs). The shapefiles for MPAs and the CCA were obtained from the

California Department of Fish and Game and the shapefiles for NMSs were obtained from the

National Oceanic and Atmospheric Administration (NOAA).

Results

<u>Lander Performance</u>

Both the Picolander and the Nanolander were found to be reliable systems for deployment, recovery, and data collection. Eleven deployments were successfully conducted (six with the Picolander and five with the Nanolander), one deployment failed and an early Picolander was lost. Small boats were used for the deployment and recovery of both landers, and they were easy to transport by either lab cart or car. The structure of the landers showed little signs of wear, even after multiple deployments. With the retrofitted camera system, used in both landers, and new lights, power consumption was consistent and predictable. A map of deployment locations is provided in figure 5.

The limitation to the Picolander's deployment length was the timed-release system. The timers currently installed have a maximum duration of 99 hours (~ 4.13 days). The next limiting factor would have been the battery capacity to run the lights. The bench battery test resulted in the LiPo battery running out of power at ~6.89 days of recording at 20 s every 20 min (496 video clips). Recovery of the Picolander is straightforward as the timers are programmed to go off at a predetermined time prior to deployment. Once the timers go off the burnwires take ~15-20 min to burn and then the Picolander ascends through the water column at a rate of ~60 m min^{-1}. Upon arriving to the surface, the Picolander floats vertically in the water column with ~1/2 of its top sphere out of the water (Fig. 3c). This combined with the flag aid in the visual detection of the lander upon surfacing. It also allows the GPS unit (Spot Trace) housed in the top hemisphere of the upper sphere to connect to satellite and notify the primary user of its location. The GPS unit was installed as a precaution if the lander came up unexpectedly or if it moved significantly during the deployment or recovery. The timed-release system worked reliably throughout the

deployments, however, one Picolander was lost. Although unconfirmed, the leading hypothesis is that the lander may have become caught under large overhanging rock segments present in the area.

The limitation on the Nanolander system's deployment length was power to the GoPro Camera. The V50 Voltaic Systems battery pack is only used to power the GoPro camera and is independent of the battery pack used for the LED lights. The V50 battery pack ran out of capacity to power the GoPro at ~ 10 days when recording for 20 s every 20 min (723 video clips). The next limiting factor for the Nanolander would have been power to the LED lights from the LiPo batteries. However, upon recovery from Nano-D170 (the longest deployment) the LiPos had ~30% battery life remaining. With 30% battery life the LiPos could have run the LEDs for approximately 4 more days recording at the same interval. The acoustic communication system was reliable during all deployments and allowed for smooth recoveries.

The Moana TD1000 Temperature and Depth sensor, which was installed on both landers, worked without any issues throughout all deployments and had sufficient power and memory capacity for all deployments.

Environmental Variability

Variability of environmental parameters were assessed using time series from all Picolander and Nanolander deployments and compared across depths (100, 200, 300, 400, and 500 m). Means and ranges for temperature and depth are provided in tables 1 and 2. Environmental data for Nano-D500 are not available as the SBE MicroCAT-ODO that was previously installed on Nanolander *DOV BEEBE* was deployed with the lander rather than the Moana TD1000 and ran out of battery power shortly after the lander was deployed. Timeseries of

depth colored by temperature for each deployment, except for Nano-D500, are provided in Fig. 6. Over the course of the Nanolander deployments, the largest tidal range (indicated by the largest differences in depth recorded by the Moana pressure sensor) was observed during the 100 m deployment (Nano-D100) (3.70 m delta) and the largest temperature range was observed during the 300 m deployment (Nano-D300) (1.29°C delta). During the Picolander deployments, the largest change in depth and in temperature were observed during the 300 m deployment, 5 m and 1.28°C deltas, respectively.

Characterizing Differences in Seafloor Community Diversity

Community data were collected over five Nanolander deployments and six Picolander deployments using the camera system. Over the course of the Nanolander deployments, 3,183 20-s video samples were annotated, and 614 20-s samples were annotated from the Picolander deployments (Table 1; Table 2). Over the course of all the deployments, visibility was worse than expected due to turbidity in the water column. The 300 m deployment had the poorest visibility, where only 9% of samples had good visibility. The 100 m deployment had the best visibility followed by the 500 m deployment, the 400 m deployment, and finally the 170 m deployment (Table 1; Table 2).

Despite having the poorest visibility, the highest number of unique OTUs (invertebrates, vertebrates, and demersal fishes) were observed at the 300 m site with 27 OTUs recorded over the course of the Nanolander deployment and 16 recorded over the course of the Picolander deployment. The 100 m Nanolander deployment observed the most demersal fish with 16 species observed. For both landers, the least number of OTUs occurred at the ~400 m deployment with the Nanolander observing 19 OTUs while the Picolander observed six (Table 1; Table 2).

The seafloor community at the 100 m deployments with both landers are characterized by high numbers of rockfish (*Sebastes spp.*) with the most common species in both deployments being the Halfbanded Rockfish (*Sebastes semicinctus*). The Nanolander deployment also recorded the Flag Rockfish (*S. rubrivinctus*), Olive Rockfish (*S. something*), and the Starry Rockfish (*S. constellatus*). The Picolander recorded the Starry Rockfish and the Vermillion Rockfish (*S. miniatus*) in addition to the Halfbanded Rockfish. Other commonly observed fish species by both the Nanolander and the Picolander included lizard fish (*Synodus lucioceps*), combfish (*Zaniolepis spp.*), and the Spotted Cusk Eel (*Chilara taylori*). The dominant invertebrate in both 100 m deployments were sea cucumbers. Also observed were small, white sea stars, small corals, and an anemone. The 100 m deployments in the cases of both landers were quite distinct from the other deployments (Fig. 10).

Deployments Nano-D170 and Pico-D180 targeted the 200 m depth range, however, both ended up being slightly shallow to avoid overhanging areas where the first deployment to 200 m, with Picolander *DOV JEAN*, was lost. The Nanolander deployment was dominated by eelpouts with the Black Eelpout (*Lycodes diapterus*) as the most numerous species. The Bigfin Eelpout (*Lycodes cortezianus*) and unidentified eelpouts were also recorded however, less frequently. Other commonly observed fishes include the Spotted Ratfish (*Hydrolagus colliei*), flatfish that were unable to be identified to species, and Spotted Cusk Eels. The dominant fishes observed with the Picolander was the Spotted Ratfish. Other commonly observed fish were the Spotted Cusk Eel, Copper Rockfish (*S. caurinus*), and Dover Sole (*Microstomus pacificus*). Large crabs were the most observed invertebrate, while Tuna Crabs (*Plueroncodes planipes*) were also observed in fewer numbers. A notable difference between the lander deployments is that the most common species observed with the Nanolander (Black Eelpouts) was not observed at all by

27

the Picolander at this depth. During the Nanolander deployment, the bait was taken from the lander 9 hours into the deployment however the camera was not on at the time the bait was taken. A few larger animals visited the landers while they were deployed, a Harbor Seal (*Phoca vitulina*) was observed by the Nanolander and a swell shark (*Cephaloscyllium ventriosum*) was observed by the Picolander. What appeared to be clear flatfish floating on the currents was also observed by the Nanolander and were hypothesized to be pre-settlement flatfish. These pre-settlement flatfish were not observed by the Picolander. The community at 200 m during the Nanolander deployments was unique from the 100 m deployment in ordination space but shares some space with the 300 m deployment (Fig. 10). The community at 200 m captured by the Picolander was distinct from all other depths in ordination space (Fig. 10).

During the 300 m deployments, visibility tended to be poor however, it was the most speciose deployment for both the Nanolander and the Picolander, with regards to total community (invertebrates, vertebrates, and demersal fishes). The poor visibility was due to high amounts of turbidity and sedimentation over the course of these deployments. During the Nanolander deployment, the drop arm could be observed getting buried via sedimentation. The most common fish observed during the Nanolander deployment was the Blackmouth Eelpout (*Lycodapus fierasfer*). The next most common species include the Black Eelpout, Dogface Witch Eel (*Facciolella equatorialis*), and small flatfish that were unable to be identified down to species. The dominant fish observed by the Picolander were the Black Eelpout. Other frequently observed fish included the Blackbelly Eelpout (*Lycodes pacificus*), Blackmouth Eelpout, and Dogface Witch Eels. The invertebrates at 300 m were dominated by crabs. The Nanolander also observed two kinds of crabs as well as two kinds of octopi, the Picolander only observed one kind of crab. Both landers observed a few kinds of jellyfish as well. The bait for the Nanolander

deployment was taken whole within 20 min of the start of the deployment. The first sample recorded by the lander is a Prickly Shark (*Echinorhinus cookei*) eating all the bait off the drop arm. The pre-settlement flatfish were also recorded at this depth only by the Nanolander. The community at 300 m overlaps with both the ~200 m community as well as the ~400 m community, potentially showing a transition zone between shallower and deep-sea communities (Fig. 10).

The ~400 m deployments were both dominated by Dogface Witch Eels. The other commonly observed fish species by the Nanolander included Blackmouth Eelpouts, hagfish (*Eptatretus stoutii*), Brown Catshark (*Apristurus brunneus*), Pacific Dover Sole, and the Pacific grenadier (*Coryphenoides acrolepis*). Flatfish that were unable to be identified to species were also frequently observed. Other commonly observed fish species by the Picolander include the Slender Sole (*Lyopsetta exilis*), Dover Sole, and Stripefin Poacher (*Xeneretmus ritteri*). The dominant invertebrate was a crab with very long legs. Octopus and several kinds of jellyfish were also observed at this depth. The community at the Nanolander's 400 m deployment overlaps slightly with the 300 m community but is distinct from the 500 m community whereas the community observed by the Picolander overlaps with both the 300 m and the 500 m community, however, at different locations in ordination space (Fig. 10).

The fish community at 500 m was dominated by flatfish in both the Nanolander and Picolander deployments with the most observed species during both deployments being the Slender Sole. Other than flatfish, Dogface Witch Eels were recorded frequently in both lander deployments. During the Nanolander deployment, the Pacific Hagfish and the Black Hagfish (*Eptatretus deani*) were very common species however, they were not observed during the Picolander deployment. This is likely due to the presence of bait on the Nanolander deployment.

Spotted Ratfish were observed at 500 m only during the Picolander deployment. The most common invertebrate at this depth were sea stars; there were often large groups (>10) in the video frame. Other observed invertebrates included octopus, large crabs, and several kinds of jellyfish. The seafloor community at 500 m during the Nanolander deployment was distinct from all other depths. The community at 500 m during the Picolander deployment had a small degree of overlap with the 400 m site but was distinct from all other depths (Fig. 10).

A deployment to 370 m was only conducted by the Picolander. The targeted depth was 400 m, however, the deployment ended up being shallower. As a result, another deployment was conducted with the Picolander at ~ 400 m and this site was revisited by the Nanolander. The 370 m deployment observed very few species overall with the community being nearly 50% Blackmouth Eelpouts (Fig. 12). Dogface Witch Eels also accounted for a large portion of the community, however, only five fish species were observed. The drop in diversity between the 300 m deployments and the 370 m deployment could be in part explained by the visibility. The 370 m deployment had consistently poor visibility. In ordination space, the 370 m deployment overlaps significantly with the 300 and 400 m deployments (Fig. 10a, c).

Differences in community diversity between deployments was examined for each lander using species accumulation curves created using video samples. For both landers, the most speciose deployment was at 300 m followed by the 100 m deployment. Then for the Nanolander deployments, the 200 and 500 m deployments had the same number of unique species, though fewer are captured if only the visibility A and A- samples are used for the accumulation curves. Finally, the 400 m deployment captured the least number of unique species (Fig. 7a, b). For the Picolander deployments the 100 m deployment captured the most species then the 180 m, 500 m, 400 m, and finally the 370 m deployment with the least number of unique species (Fig. 6c). At

all depths, the Nanolander observed more unique species than the Picolander, this is likely due to the longer deployment time of the Nanolander (Fig. 7, Table 1, Table 2).

Characterizing Differences in the Demersal Fish Community

During the 500 m Nanolander deployment, Slender Soles accounted for ~26% of the demersal fish community and were the most abundant demersal fish observed throughout the deployment. The most abundant demersal fish in the 400 and 300 m deployments were Dogface Witch Eels which accounted for ~ 35% of the community in both Nanolander deployments. Black Eelpouts accounted for ~50% of the demersal fish community in the Nanolander's 170 m deployment. And in the 100 m deployment Halfbanded Rockfish accounted for the largest proportion of the community (~36%). The communities captured by the Picolander followed similar trends, though the proportions are different. This could be due to the difference in deployment length or the lack of bait.

The inverse Berger-Parker index followed an increasing trend from 100 m to 300 m then declined at 400 m and rebounded to its maximum at the 500 m deployment (1.917). Indicating that the 500 m deployment had the least dominance (most evenness) in the demersal fish community (Table 4). A similar trend was observed in the species richness with the values increasing from 100 to 300 m, however, the maximum value for mean species richness occurred at 300 m (6.264). Then the mean species richness declined at 400 m to 4.647 and increased slightly to 4.828 at 500 m (Table 4).

Diurnal Patterns

Diurnal patterns of common fish species were assessed using count data from video samples collected by the Nanolander and Picolander (Fig. 13). Only data from deployments where these species were observed were used. Dogface Witch Eels (*F. equatorialis*) showed a

nocturnal pattern with more frequent observations at night, and the strength of this signal

increased at shallower depths (Fig. 13d). In contrast, Blackmouth Eelpouts (*L. fierasfer*), Black

Eelpouts (*L. diapterus*), and Halfbanded Rockfish (*S. semicinctus*) showed diurnal patterns with

more common observations in the day (Fig. 13a-c). The strength of the signal for both the

nocturnal and diurnal patterns behaved as hypothesized and increased with shallower depths. The

larval flatfish were only observed during two Nanolander deployments, at 170 m and 300 m

(Nano-D170, Nano-D300). During the 300 m deployment, the larval flatfish were only observed

during the day. While during the 170 m deployment, the larval flatfish were only observed at

night (Fig. 13e).

Due to the diurnal patterns of the common species, community differences between day

and night were assessed for each depth using the video samples from the Nanolander and the

Picolander. Additionally, only Nanolander samples with A or A- visibility and lander samples

with organisms present were used. The 100 and 300 m deployments showed clear differences in

the community between day and night (Fig. 14a, c). Contrary to our hypothesis, the community

at 170 m did not show much difference between the daytime and nighttime communities (Fig.

14b). The 400 and 500 m deployments also showed little differences in the community between

day and night (Fig. 14d, e).

Comparing Lander Results to the Marine Vertebrate Collection at SIO

Over the course of all lander deployments 40 species of fishes were identified. The list of

local canyon fish species preserved in the MVC adapted from Hastings et al. (2014) included 98

species of fish. When these lists were compared, the lander deployments observed 19 of the

preserved fish species, ~ 20% of the list. However, the other 21 species observed by the landers

were not logged in the collection as being canyon associated, ~53% of fish species observed by

the lander (Fig. 15). A complete list of the fish species preserved in the MVC and observed by the landers is provided in the appendix (supplementary table 1).

Identifying Small Submarine Canyons

Small submarine canyons were identified using Arc-GIS Pro software with methods adapted from Harris et al., 2014 (Fig.4). Small submarine canyons were defined as canyons that extend to a minimum depth of 200 m and incised into the slope at least 100 m. By applying this definition, 23 small submarine canyons were identified along the coast of southern and central coast of California. These were grouped into one of three categories: nearshore (within 5 km of coastline), offshore (not within 5 km of coastline), and extension of a large canyon (a section of a larger canyon from Harris et al., 2014). Of the 23 small submarine canyons identified, 10 were classified as nearshore submarine canyons, 6 were classified as offshore canyons, and 7 were classified as nearshore extensions of larger canyons (Table 4).

Protection of Submarine Canyons off the Coast of California

We found that of the 23 small submarine canyons identified in this study, 7 had some of their area overlap with a protected area. The 23 small submarine canyons along the coast of California were found to have a total area of 871.49 km^2. The area protected for this size class was found to be 196.49 km^2, or 22.55% of the total area. From the Harris et al., 2014, dataset 51 large submarine canyons were identified along the coast of California. These large canyons have a total area of 25,736.84 km^2. We found that of the 51 submarine canyons, 24 intersect at some point with a protected area. For this size class, an area of 7,140.37 km^2 fell within protected areas, or 27.74% of the total area. In both size classes of canyons, most of the area that was protected fell into an NMS. CCAs protected the second largest portion of the large canyons

followed by the MPAs. For small canyons, CCAs did not protect any of their area. As a result,

the MPAs protected the second largest portion (Table 4; Fig. 17).

Discussion

<u>Canyon and Ecological Findings</u>

We found that nearshore submarine canyons are areas of increased turbidity, especially at depths between 300 and 400 m, similar to that observed off the coast of Del Mar where a sharp dip in visibility conditions occurred at about 360 m (Gallo et al., 2016). Internal waves are the primary drivers of environmental variability in the La Jolla Canyon (Hamann, 2019) and we hypothesize that the stretches of time with reduced visibility at depth are due to particularly strong internal waves at that time.

Despite having some of the poorest visibility conditions, the 300 m deployment with the Picolander recorded the highest number of unique operation taxonomic units (OTUs) of both invertebrates and vertebrates and the highest number of demersal fishes observed by that lander. The Nanolander also observed the most unique OTUs at 300 m, however, the most demersal fishes were observed at 100 m (Table 1; Table 2). We expected to see have the highest degree of diversity at the shallower deployments, and it was surprising that diversity was highest at 300 m. The mean species richness per sample was also the highest at 300 m. The deployments with the lowest biodiversity were the 400 m deployment by the Nanolander and the 370 m deployment by the Picolander. The extremely low diversity during the 370 m deployment is likely due to the poor visibility at that depth. We hypothesize the low diversity observed at 400 m to be due to low oxygen conditions. The Nanolander study conducted in 2016 found severely hypoxic conditions at ~400 m on the upper margin (Gallo et al., 2020). Submarine canyons tend to approximate local oxygen gradients; therefore, it is possible that severely hypoxic conditions occur in the canyon at ~400 m.

Comparing our community results to a similar study conducted off the coast of Del Mar at the Del Mar Steeples Reef just slightly north of our study area and outside of the canyon area, many of the same species were observed (Gallo et al., 2018). During the 100 m deployments at both locations, the most abundant species were similar with both sites dominated by benthic eelpouts and rockfish. Additionally, the observation of very few bait attending species at 100 m was common between both locations. The study conducted off Del Mar had two different ~ 200 m deployment locations, one near a canyon tributary and the other closer to the Del Mar Steeples Reef. The deployment closer to the canyon observed many of the same species that were recorded during this study. However, the deployment conducted closer to Del Mar Steeples Reef recorded very few of the same species, with that deployment more closely resembling the 100 m location in the canyon. The ~ 300 m deployment location for the Del Mar study was conducted near the Del Mar Steeples Reef, away from the canyon. Like the lander deployments from this study, the visibility at this location was very poor. However, unlike the lander deployments from this study the diversity at Del Mar Steeples Reef at the 300 m location was the lowest observed over the course of that study. The deepest deployment conducted by the study done at Del Mar was at 400 m away from the canyon edge. This deployment had many of the same fish species as the canyon deployments at a similar depth however, very commonly observed large numbers of Pink Sea Urchins (*S. fragilis*). In contrast, Pink Sea Urchins were not observed at all over the course of the canyon deployments. Overall, the Del Mar Steeples deployments observed many more Tuna Crabs (*P. planipes*), Pink Sea Urchins, and crabs (*Cancer spp.*) than were observed in the canyon deployments, with several of the Del Mar deployments dominated by one of those species.

The ordination plots revealed that the communities in the 100 m and the 500 m deployments were quite distinct from all others (Fig. 10). The 300 m deployment appeared to be a transition zone between the ~200 m deployments and the 400 m deployments. This is supported by the Picolander deployment to 370 m which was placed as a transition between the 300 m and 400 m communities. We hypothesize that 300 m is a transition zone in the canyon between shallow and deep-sea communities and that this is a contributing factor to the increase in number of OTUs recorded at this depth. This is further supported in that the demersal fishes proportion plot (Fig. 11), the community at 300 m was made up of fishes common at both 200 m and 400 m.

The demersal fish community was most even in the 500 m Nanolander deployment seen in the species proportion barplot (Fig. 11) as well as the inverse Berger-Parker index of dominance that was the highest at 500 m which is indicative of a low degree of dominance. The deployment with the least even (most dominant) demersal fish community was the 100 m deployment. This deployment was dominated by Halfbanded Rockfish. The highest percentage of samples with no demersal fish was at 100 m with the Nanolander. This could have been artificially inflated by the position of the lander on the edge of a drop off with rocky reefs on either side. Demersal fishes could be seen swimming around rocks and into crevices but when the lander was facing the drop off, the small rocky reefs were not visible.

A notable difference between the Nanolander and Picolander deployments is that during the 170 m Nanolander deployment, Black Eelpouts accounted for almost 50% of the demersal fish community however, they were not observed at this depth by the Picolander. The Picolander only observed Black Eelpouts at 300 m, and they accounted for a large proportion of the demersal fish community at this depth. This could potentially be a seasonal movement of Black

Eelpouts as the deployments were conducted ~4 months apart with the Picolander deployment in November and the Nanolander deployment in April. The temperatures for these deployments were examined to see if the range overlapped significantly. However, the temperature range overlap is small leading to the idea that Black Eelpouts may have different temperature and/or depth preferences at different times of year.

We were able to observe diurnal patterns of common species as well as communities at the different depths. We found that some common species follow a diurnal pattern and that the pattern is stronger at shallower depths (Fig. 13). A unique observation that we made was regarding the larval flatfish (Fig. 13e). The larval flatfish were only observed during two, consecutive Nanolander deployments, to 300 and 170 m. They were only observed during the day at 300 m and only observed during the night at 170 m. We hypothesize that this may be due to diel vertical migration of these larvae.

It is interesting to note that the species with the clearest diurnal patterns were observed at depths deeper than 300 m. This is an interesting observation as we expected the diurnal patterns of species to decrease with depth and be most obvious at the shallower deployments. However, the Black Eelpout and Halfbanded Rockfish (most common species at ~200 m and 100 m respectively) showed very weak diurnal patterns (Fig. 13). This could be due to their sedentary nature. In the future, it would be interesting to note activity levels and compare the diurnal patterns between when the fish are more active and when they are more sedentary.

When the communities were analyzed with respect to diurnal patterns, the 100 m deployment showed the largest difference between day and night (Fig. 14). This was the only deployment, however, that showed a very clear pattern. This contrasts with previous work done

off the coast of Del Mar (Gallo et al., 2018) where significant diurnal differences in communities at 200 m and especially 100 m were observed.

Comparing Lander Results to the Marine Vertebrate Collection at SIO

The landers recorded 40 species of fishes throughout their deployments and ~47% of these were also preserved in the MVC at SIO and collected from the local canyon system (Fig. 15). The remaining ~ 53% of the fish species observed by the lander were not preserved in the MVC with metadata indicating that they were collected from the local canyon system. It is possible that the disparity between what has been collected from the canyon and what was observed by the lander is due to the different data collecting methods. Most of the samples from the local canyon system in the MVC were collected using rotenone or dynamite. It is possible that the species only observed by the landers were less susceptible to these methods or did not float up to the surface to be collected. Additionally, the specimens in the MVC were collected over several decades ago and the difference in species observed by the landers and preserved in the MVC could be evidence of a change in the system. It is worth considering this possibility however, more extensive ecological sampling of the canyon is required. This result supports the need for more and diverse sampling efforts in ecological research and proves efficacy of the landers as tools to study nearshore submarine canyon communities.

Submarine Canyon Protection

Off the coast of California, we found that there were 23 small, nearshore submarine canyons. Of those 23 small canyons, ten were further classified as nearshore submarine canyons and seven as extensions of larger canyon features. Of the ten small, nearshore submarine canyons identified only three intersected with a protected area for a total of 3.21% of their area receiving protection. We noticed when conducting this analysis that it is only the onshore reaches of these

canyons that intersect with protected areas (Fig. 17) often leaving the offshore reaches without protected status. This trend was also reflected in the small canyons that did have protection. Due to strong flows along the canyon axes, I propose it would be beneficial to protect more of the offshore reaches of the submarine canyons. These axes-long flows can carry pollution that is dumped on the offshore reaches of the canyon up and into the nearshore areas some of which may intersect with protected areas. Or conversely, garbage can be taken from unprotected nearshore areas and deposited in sensitive deep-sea habitat.

It is extremely difficult to make informed management decisions about an area where we have a limited understanding of the ecology and a lack of baseline knowledge. Canyons are important ecological features providing hunting grounds for large predators, refuge for juveniles and keystone structures for nearby fisheries. As coastal waters continue to warm due to climate change, they may also provide climate refugia to coastal species as the deep water will stay a cooler temperature than the shallow water of the slope. Collecting baseline data on these areas can provide a reference point to see what is changing due to anthropogenic effects or due to climate change. Without baseline knowledge, there is no way to understand if the protection measures in place are effective or how disturbed an area has become.

<u>Lander Performance</u>

Due to their small design and relative ease of use, small autonomous landers such as the Nanolander *DOV BEEBE* and Picolander *DOV LEVIN* can greatly increase the access to nearshore, deep-sea ecosystems. We found the landers performed reliably and were valuable tools for collecting paired biological, physical, and biogeochemical data in hard to access areas. Because of this, they can serve as powerful tools to investigate a great diversity of questions from animal behavior to community responses to the environment.

The Picolander design proved to be a good tool for short-term exploratory deployments. The limiting factor for how long the Picolander could be out for was the timed-release system. The timers could only be set to 99 hours. If an acoustic release system were added that time could be extended. The next limiter for the Picolander would be power to the LED lights. With the one onboard LiPo battery, the camera and lights system can have sufficient power for 7 days.

The Nanolander design continued to function reliably, and the retrofitted camera system accomplished the goals we had for power conservation. The maximum amount of time we got out of the Nanolander camera system was 10 days, limited by the power to the camera via the Voltaic battery. Because the power systems are independent, only a minor modification of adding an additional Voltaic battery pack or incorporating a single higher capacity battery pack could extend the deployment length for the Nanolander by 30-40%. In addition to adding more power capacity, the GoPro camera and CamDo Timelapse controller could be updated to a newer model to achieve higher quality video.

The Nanolander was equipped with a payload bay that was about half of its height. This payload bay was originally added to the design in order to accommodate additional instrumentation. While this is an extremely useful feature, we did not have any additional instrumentation for the purposes of this study, and it would have been useful to have the payload bay be a modular piece of the instrument. The capability to add or remove a payload bay to a lander would provide greater flexibility with regards to size and ease of use.

Both landers performed very well in the canyons, however, turbidity at depth was much higher than expected. Low visibility has a large impact on the quality of data from a video system. The addition of a hydrophone to the lander would provide additional sampling capabilities even in poor visibility conditions.

Future work for the landers could be expanded into additional hard to access areas including remote deep-sea locations, fjords, or remote locations in general. Due to their small size, they are relatively easy to transport using a car or on a plane. In addition to monitoring hard to reach environments, lander can be mobilized very quickly. This could lead to them being a valuable tool in monitoring strong upwelling events that come up quickly and have a large effect on local conditions. Expanding a fleet of small autonomous landers could be a useful way to greatly increase our knowledge of seafloor communities under a great variety of conditions and locations.

Tables

Table 1: Information for all six deployments conducted with the Picolanders *DOV JEAN* and *DOV LEVIN* including deployment dates, length, location, depth, temperature, and details about the samples collected. A sample is one 20-s video clip recorded by the lander. Only deployment Pico-D90 was conducted with *DOV JEAN*, all other deployments were conducted with *DOV LEVIN*.

	Pico-D500	Pico-D425	Pico-D370	Pico-D300	Pico-D180	Pico-D90
Dates	Oct. 29 - 30, 2020	Oct. 22 - 23, 2020	Oct. 7 - 9, 2020	Nov. 17 - 18, 2020	Dec. 16 - 18, 2020	July 22 - 23, 2020
Deployment Duration (hours)	27	26.5	50.7	26.4	50.8	25.8
Location	32.9021°N, -117.3234°W	32.8911, -117.3086	32.8840, -117.2875	32.8686, -117.2781	32.8712, -117.2645	32.8853, -117.2801
Bottom Depth (m)	492.3	425.4	368.2	301.6	180.1	90.14
Depth Range (m)	491.2 - 493.3	424.3 - 426.2	367.2 - 369.2	298.2 - 303.2	178.2 - 181.5	88.40 - 91.60
Mean Temp (°C)	6.500	7.065	7.596	8.300	9.636	10.37
Temp Range (°C)	6.386 - 6.888	6.815 - 7.282	7.385 - 7.843	7.737 - 9.015	9.152 - 10.21	10.14 - 10.88
CV Temp (°C)	1.821	1.800	1.410	3.911	2.451	1.535
No. OTUs Observed	9	6	9	16	12	9
No. Samples	79	78	150	78	151	78
Time Total for Videos Recorded (min)	26	26	50	26	50	26

Table 2: Information for all five deployments conducted with the Nanolander *DOV BEEBE* including deployment dates, length, location, depth, temperature, and details about the samples collected.

		Nano-D500	Nano-D400	Nano-D300	Nano-D170	Nano-D100
Dates		Feb. 10 - Feb. 19, 2021	Feb. 24 - Mar. 24, 2021	Mar. 19 - Mar. 27, 2020	Apr. 1 - Apr. 14, 2021	Apr. 22 - May 5, 2021
Deployment Duration (days)		8.94	8.03	8.15	13.0	13.1
Location		32.9021, -117.3234	32.8911, -117.3086	32.8686, -117.2781	32.8710, -117.2647	32.8853, -117.2801
Bottom Depth (m)		N/A	415.6	304.0	165.6	115.5
Depth Range (m)		N/A	414.1 - 416.9	302.7 - 305.1	164.1 - 166.9	113.4 - 117.1
Mean Temp (°C)		N/A	7.457	8.186	9.521	9.726
Temp Range (°C)		N/A	6.844 - 7.867	7.505 - 8.795	8.909 - 9.941	9.448 - 10.20
CV Temp (°C)		N/A	2.377	2.928	2.068	1.382
Visibility Summary (No. Samples)	A, A-	347; 256	9; 419	1; 52	102; 377	607; 36
	B, B-	40, 4	149; 3	110; 196	181; 11	1
	C	0	0	229	48	0
No. OTUs Observed		21	19	27	21	24
No. Samples		646	580	588	723	646
Time Total for Videos Recorded (h)		3.58	3.22	3.27	4.02	3.59
No. Samples Retained for Analysis		572	240	52	378	326

Table 3: The Berger-Parker index of dominance, its inverse, and species richness for each sample where demersal fish were observed over the course of the Nanolander deployments. The mean of the sample index values and the standard deviation are given in the table as well as the mean species richness per sample. The value of the index indicates how even or uneven the community is. The reciprocal of the index, 1/d, is often used, so that an increase in the value of the index accompanies an increase in diversity and a reduction in dominance.

|	Berger-Parker Dominance		Inv. Berger-Parker Dominance		Species Richness
	$D = N_{max} / N$		1/D		
	Mean	SD	Mean	SD	Mean
Nano-D100	0.930	0.176	1.149	0.402	4.350
Nano-D170	0.783	0.238	1.438	0.559	5.200
Nano-D300	0.708	0.219	1.588	0.615	6.264
Nano-D400	0.885	0.206	1.232	0.457	4.647
Nano-D500	0.837	0.236	1.917	0.559	4.828

Table 4: Properties of small and large canyons identified in southern California including the area of each that is currently under protection. MPAs = marine protected areas; NMS = National Marine Sanctuaries; CCA = Cowcod Conservation Areas.

Canyon Size	Number	Total Area (km²)	Number Protected	Total Area Protected (km²)	% Area Protected MPAs	%Area Protected NMS	% Area Protected CCA	Percent Area Protected
Small	23	871.49	7	196.49	0.81%	21.74%	0.00%	22.55%
Large	51	25736.84	24	7140.37	0.38%	21.90%	5.46%	27.74%
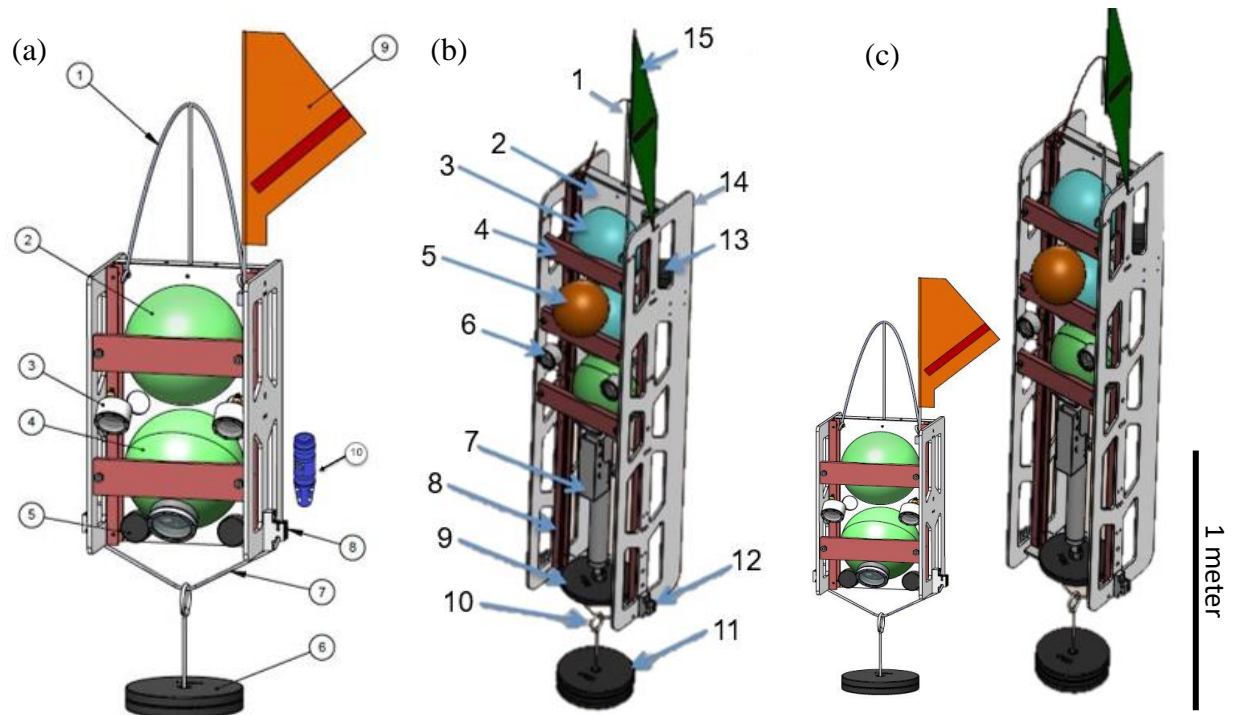
Figure 1: (a) Diagram of the Picolander *DOV JEAN*. 1) Spectra lifting bale; 2) ~25cm polyamide control sphere containing the timed-release system; 3) oil-filled LED lights; 4) ~25cm polyamide camera sphere containing a GoPro Hero 4, CamDo timelapse controller, V50 Voltaic Systems battery,16mAh LiPo battery, and battery management system; 5) 1.5lb counterweights x2 sides; 6) 25lbs expendable iron anchor; 7) chain connecting weights to the burnwires; 8) burnwire release and mount x2 sides; 9) surface recovery flag; 10) ZebraTech Moana pressure and temperature sensor (fastened to the interior of the frame. (b) Diagram of the Nanolander *DOV BEEBE* components from Gallo et al. (2020): 1) Spectra lifting bale; 2) HDPE centerplate; 3) ~25 cm polyamide spheres stacked top, middle and bottom, top is the command sphere, middle has 32mAh LiPo battery, and bottom is the camera; 4) sphere retainer; 5) auxiliary ~18 cm flotation sphere; 6) oil-filled LED lights; 7) Seabird MicroCAT-ODO in the lower payload bay; 8) central fiberglass frame; 9) stabilizing counterweight; 10) anchor slip ring; 11) 40lbs expendable iron anchor; 12) burnwire release and mount x2 sides; 13) Edgetech hydrophone for acoustic command and tracking; 14) HDPE side panels; and 15) surface recovery flag. Not shown: drop arm on front. (c) To scale images of the landers for size comparison.
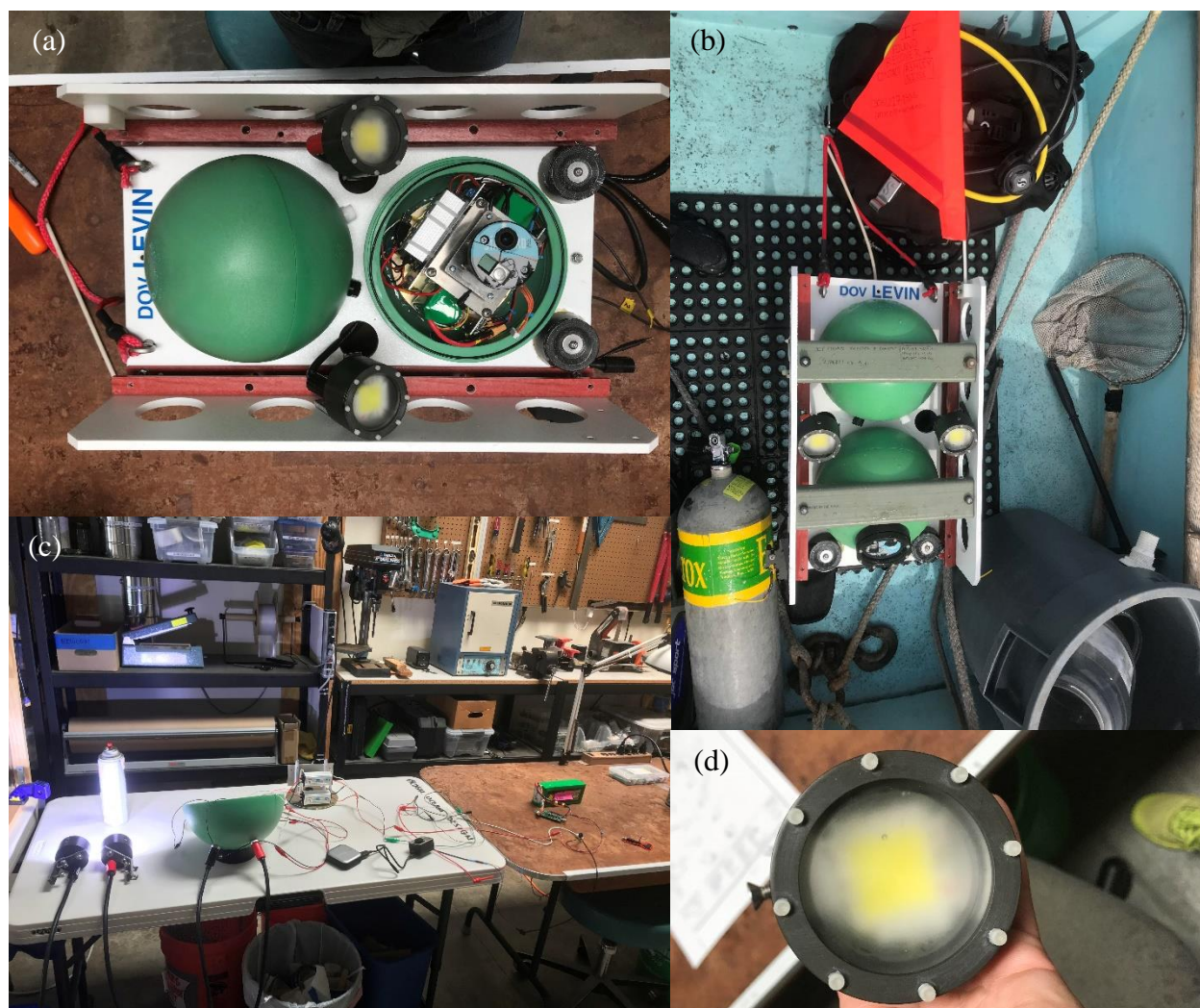
Figure 2: Pictures of the Picolander *DOV LEVIN*. The Picolander was newly designed and built for this project to be used in conjunction with the Nanolander *DOV BEEBE*. The retrofitted lights and camera were designed to be interchangeable between the two landers. a) *DOV LEVIN* with the new LED lights installed and the retrofitted camera system opened to show the inside of the sphere. b) *DOV LEVIN* on the boat after recovery. c) The camera and lights system laid out on the lab bench during a test prior to packaging it into the sphere. d) A close up of the oil filled LED lights used on both landers.
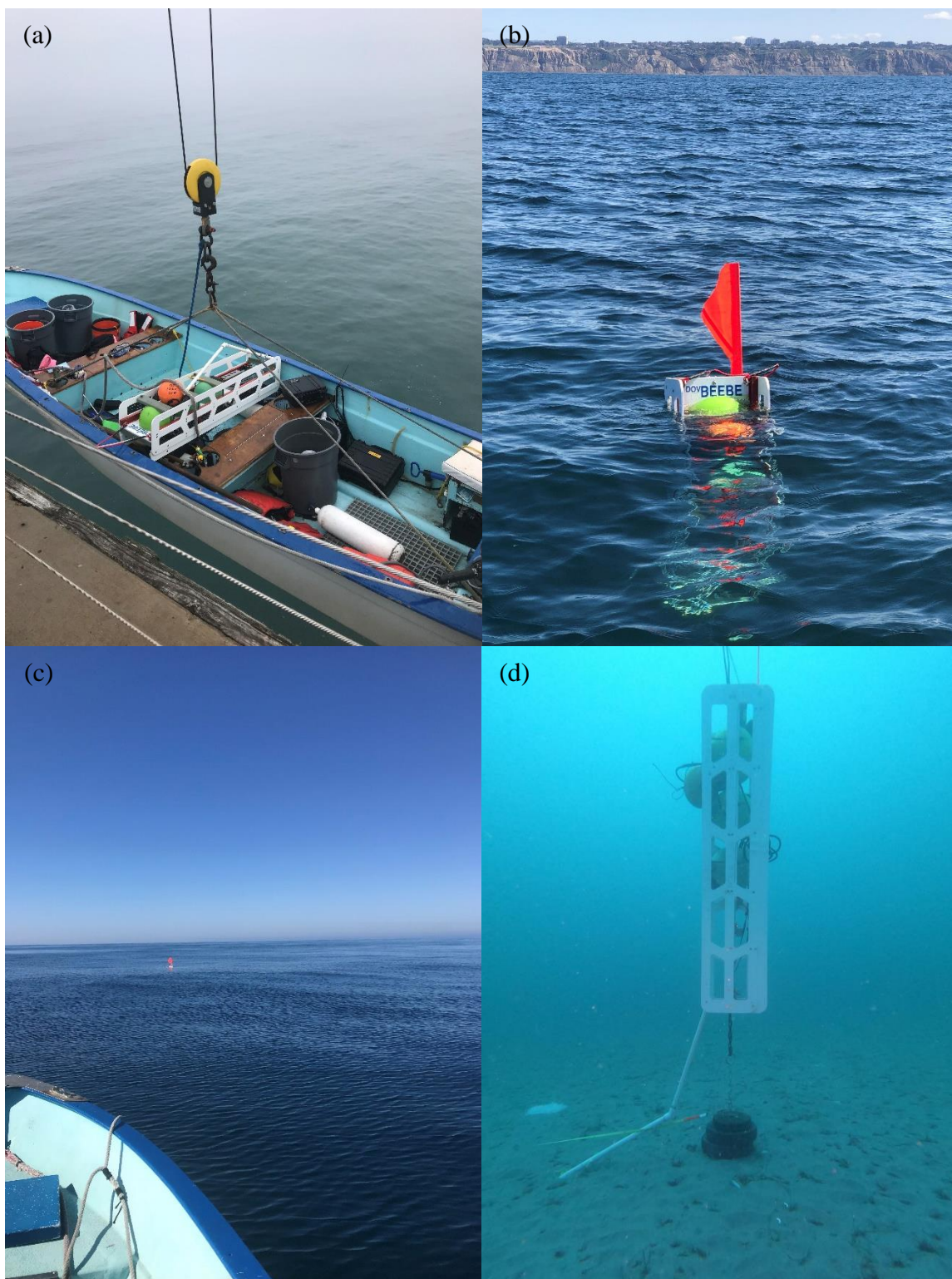
Figure 3: Photos of the landers upon deployment and/or recovery. a) Nanolander *DOV BEEBE* in a small skiff. b) *DOV BEEBE* floating in the water during a recovery. c) The surface signal of Picolander *DOV LEVIN*. d) *DOV BEEBE* deployed at ~ 24 m (80ft).
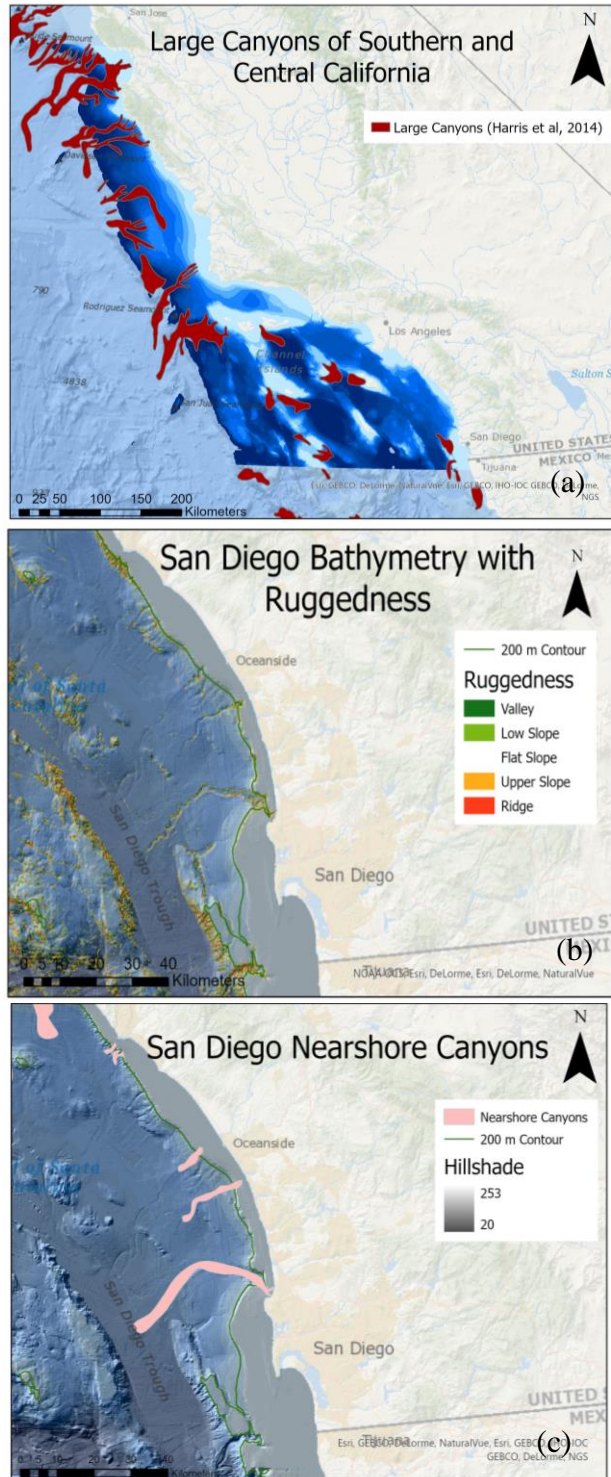
Figure 4: Process for identifying small canyons off the coast of California. a) Starting point with the bathymetry data including the large canyon data set (Harris et al., 2014). b) The San Diego area with 1-arc second bathymetry, TPI, and the 200 m contour plotted. c) The San Diego area with 1-arc second bathymetry, the newly digitized canyons, and the 200 m contour plotted.
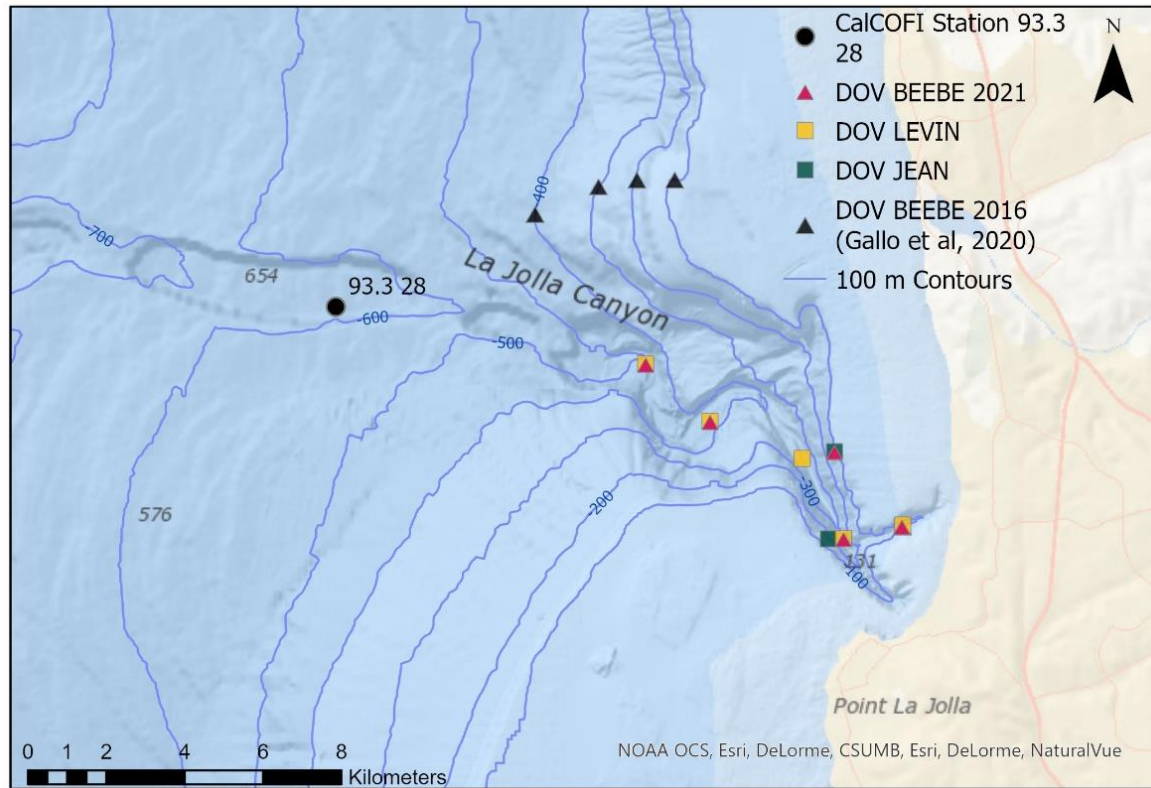
Figure 5: Map of deployment locations in or near the La Jolla Canyon with contour lines plotted every 100 m. The red triangles represent deployments conducted with the Nanolander *DOV BEEBE* in 2021, the yellow squares represent Picolander deployments conducted with *DOV LEVIN*, the green square represents the successful deployment of Picolander *DOV JEAN*, the black triangles represent the *DOV BEEBE* deployments conducted by Natalya Gallo in 2016 (Gallo, 2018; Gallo et al., 2020), and the black circle represents CalCOFI Station 93.3 28.
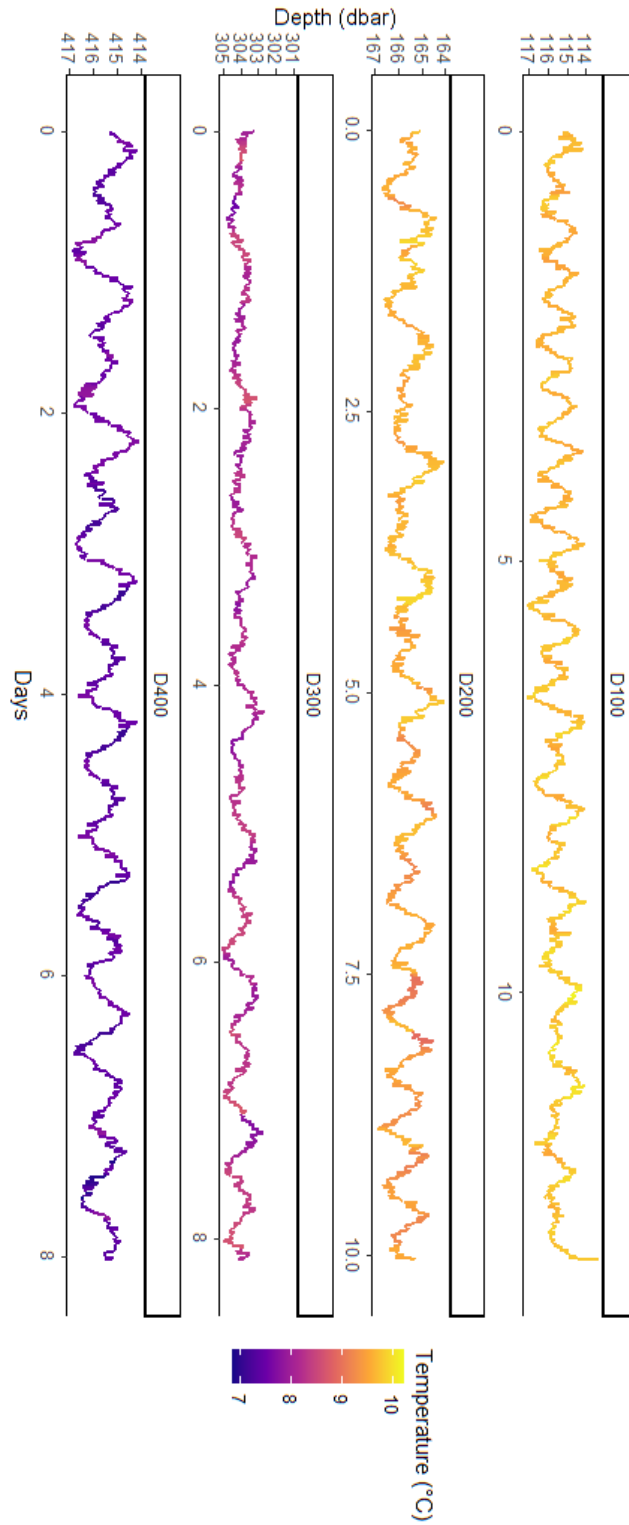
Figure 6: Timeseries showing the change in depth over time for each Nanolander deployment where temperature and depth data were collected colored by temperature (higher temperature in yellow).
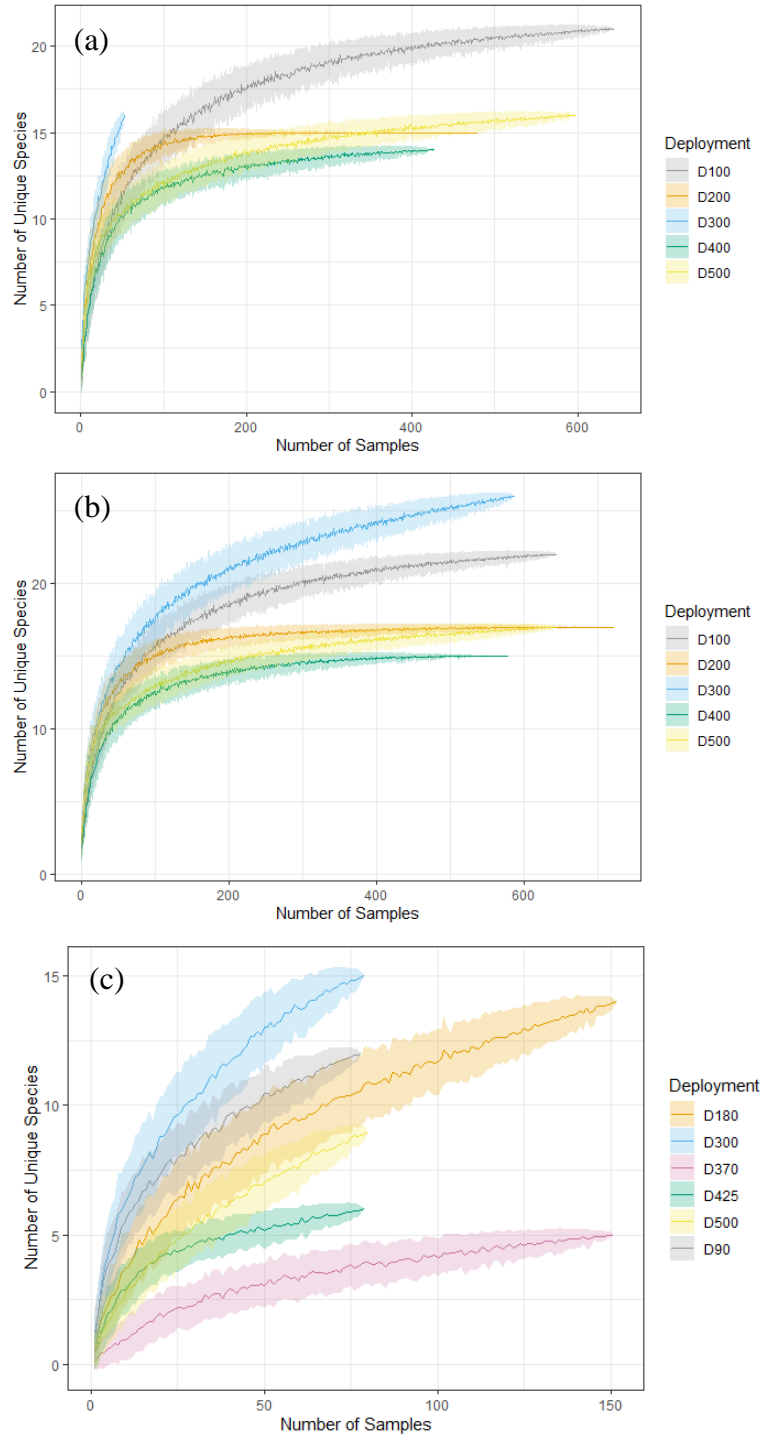
Figure 7: Species accumulation curves of all unique species (invertebrates, vertebrates, and demersal fishes) plotted against the number of 20-sec video clips. The shaded regions represent 95% confidence intervals. a) Nanolander deployments using only visibility category A or A-samples. b) Nanolander deployments using all visibility categories. c) Picolander deployments using all samples.
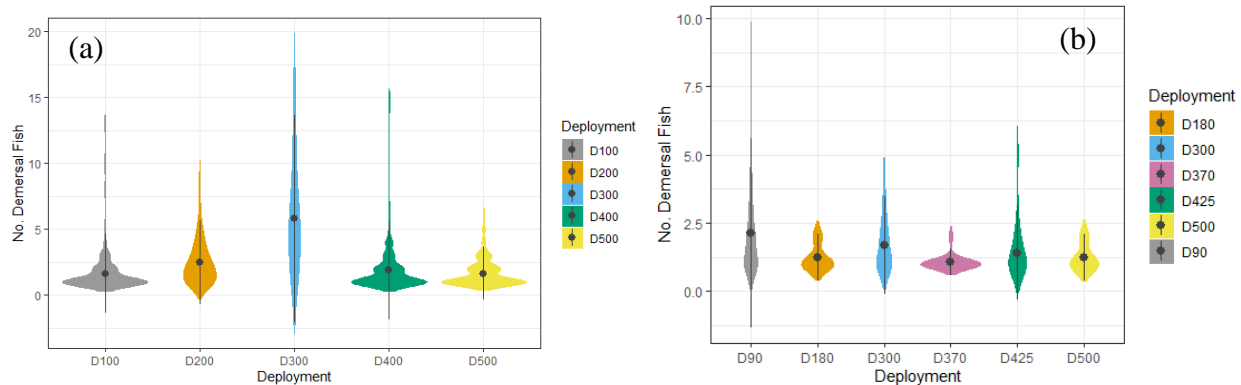
|	% A or A- Samples without Demersal Fish		
	Picolander		Nanolander
Pico-D90	26%	**Nano-D100**	70%
Pico-D180	57%	**Nano-D170**	25%
Pico-D300	28%	**Nano-D300**	2%
Pico-D370	89%	**Nano-D400**	50%
Pico-D425	63%	**Nano-D500**	30%
Pico-D500	74%		

Figure 8: Violin plots showing the number of demersal fish per video clip for deployment with A or A- visibility. 47% of Nanolander samples and 66% of Picolander samples had no demersal fish observations. a) All Nanolander deployments, b) all Picolander deployments. Table summarizing the percentage of A or A- samples with no demersal fish present by deployment.
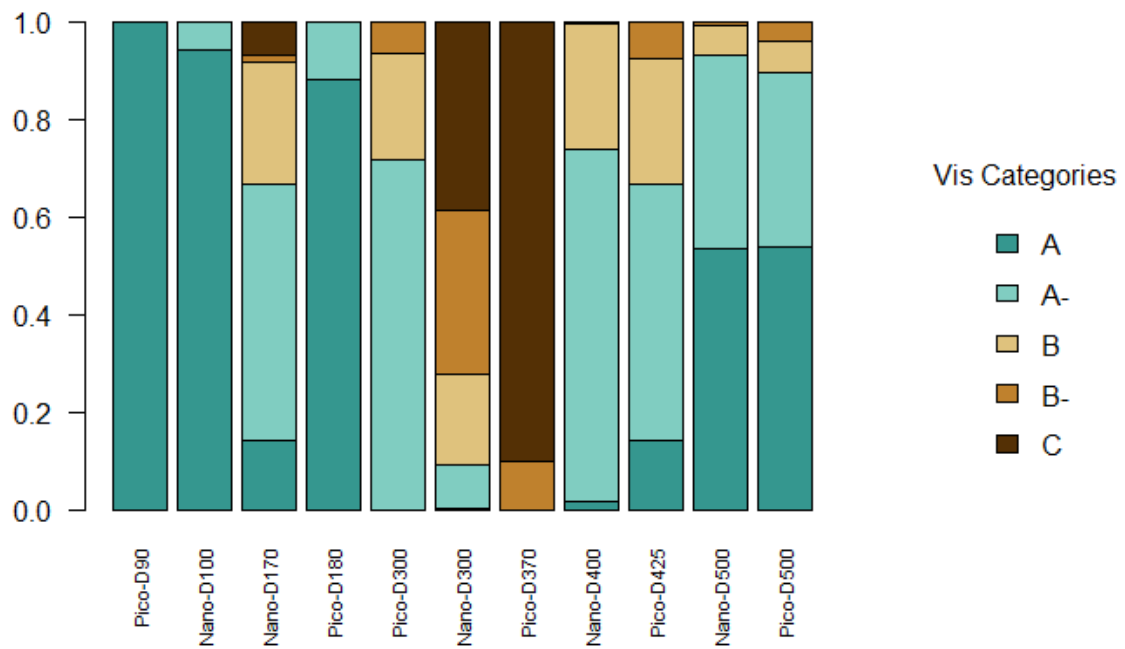
Figure 9: Barplot showing the proportion of samples of each visibility category for each Nanolander deployment. Blue represents good visibility, yellow represents intermediate visibility, and brown represents poor visibility.
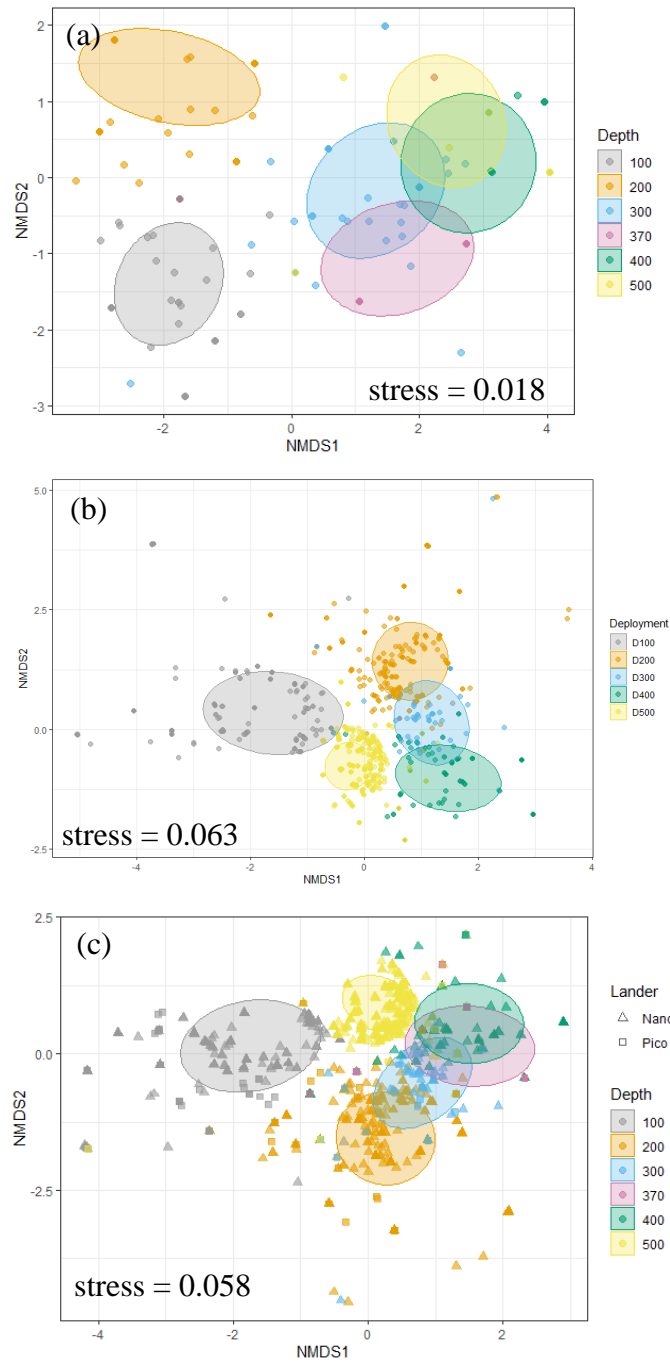
Figure 10: nMDS plots showing the differences in communities between depths. a) nMDS plot using only data collected on Picolander deployments. b) nMDS plot using only visibility A or A- data collected on Nanolander deployments. c) nMDS plot combining the data from the Picolander with the visibility A or A- data from the Nanolander; triangle points denote Nanolander data while squares represent Picolander data. Ellipses represent grouping category and 50% confidence limits.
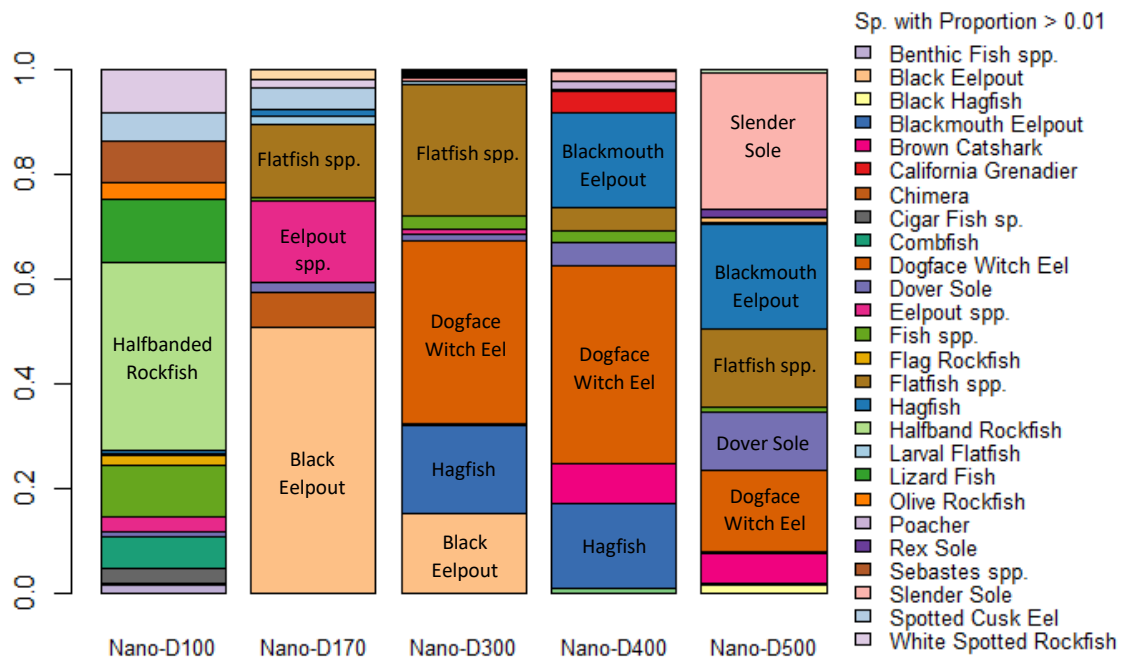
Figure 11: Community composition changes with depth captured by the Nanolander. The balance of the demersal fish community is illustrated with the barplots using video data from the Nanolander deployments. Only data with visibility category A or A- was used for this analysis. The legend shows fish species that account for at least 1% of the community for at least one deployment.
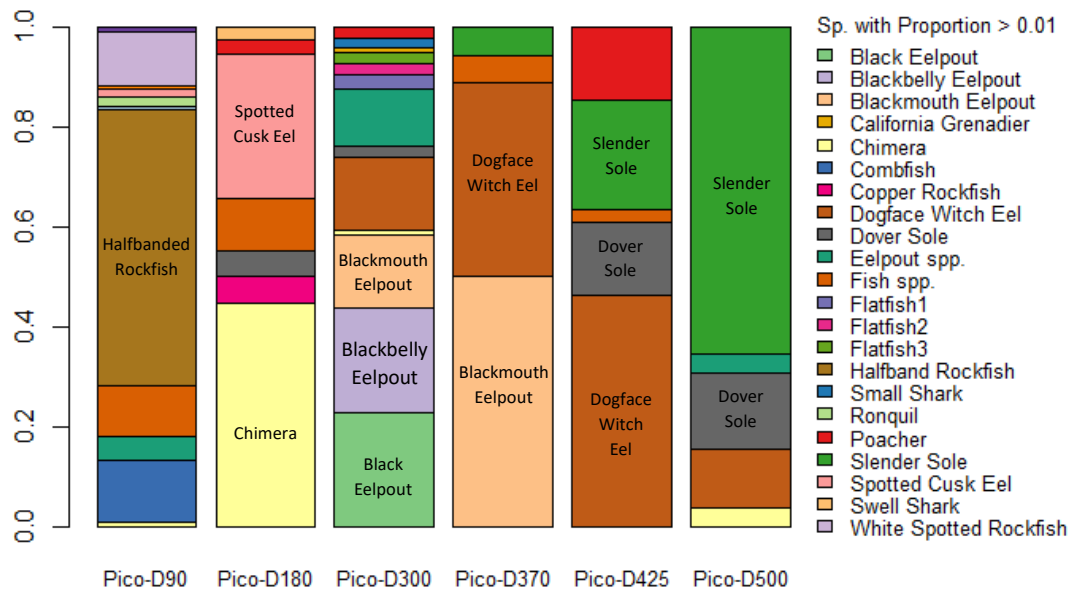
Figure 12: Community composition changes with depth captured by the Picolanders. The balance of the demersal fish community is illustrated with the barplots using video data from the Picolander deployments. The legend shows fish species that account for at least 1% of the community for at least one deployment.
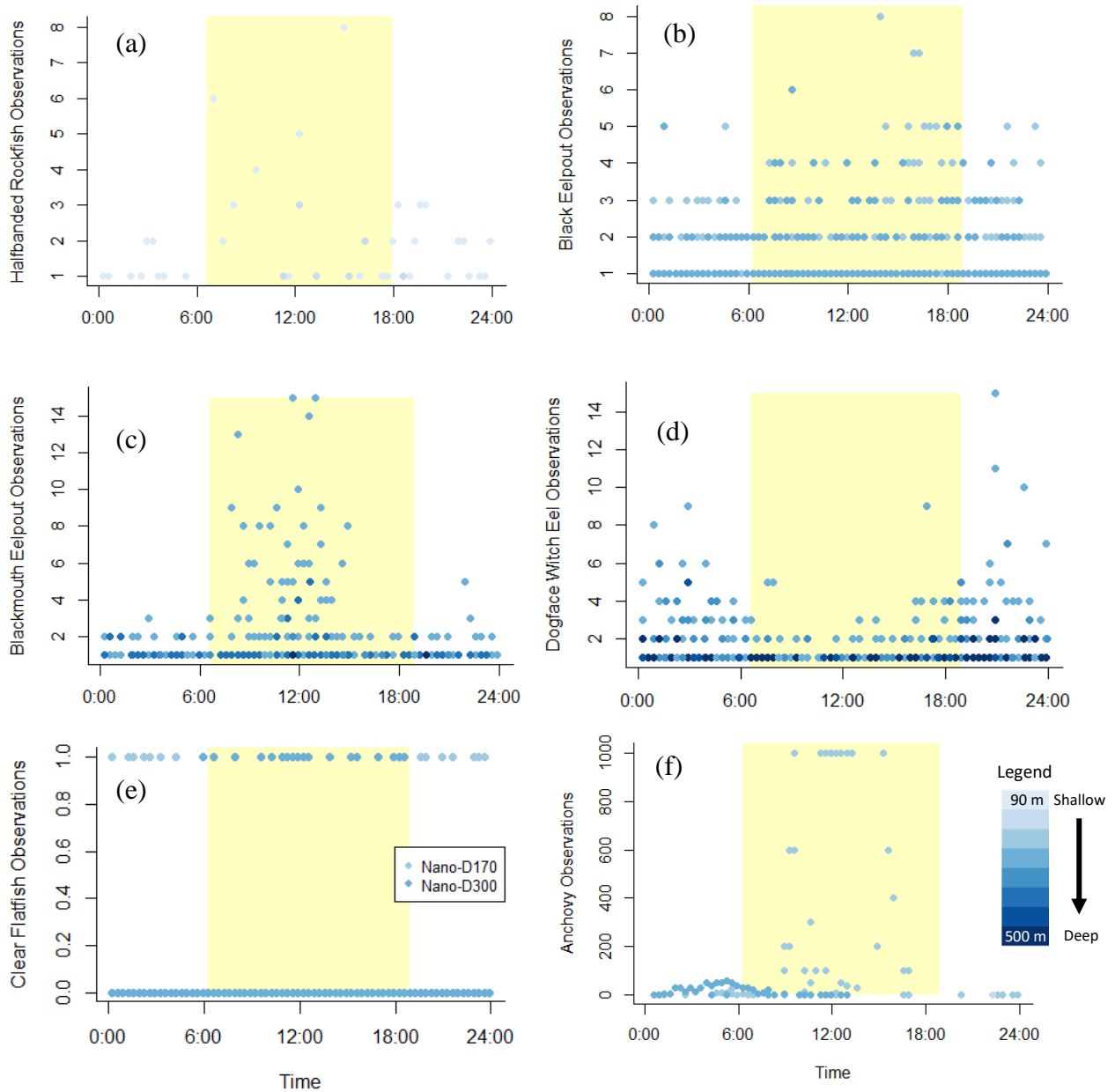
Figure 13: Diurnal behaviors based on count data collected from all deployments where these species were observed. Hours between 0600 and 1759 were considered "day" and are shown inside the yellow box. Points represent counts of each animal observed during 20 second video segments at different times of day, pooled across the length of the whole deployment and are colored by depth. Lighter blues represent shallower depths while darker blues represent deeper depths. a) Halfbanded Rockfish (*Sebastes semicinctus*), b) Black Eelpouts (*Lycodes diapterus*), c) Blackmouth Eelpouts (*Lycodapus fierasfer*), d) Dogface Witch Eels (*Facciolella equatorialis*), e) larval flatfish, f) anchovy (*Engraulis mordax*).
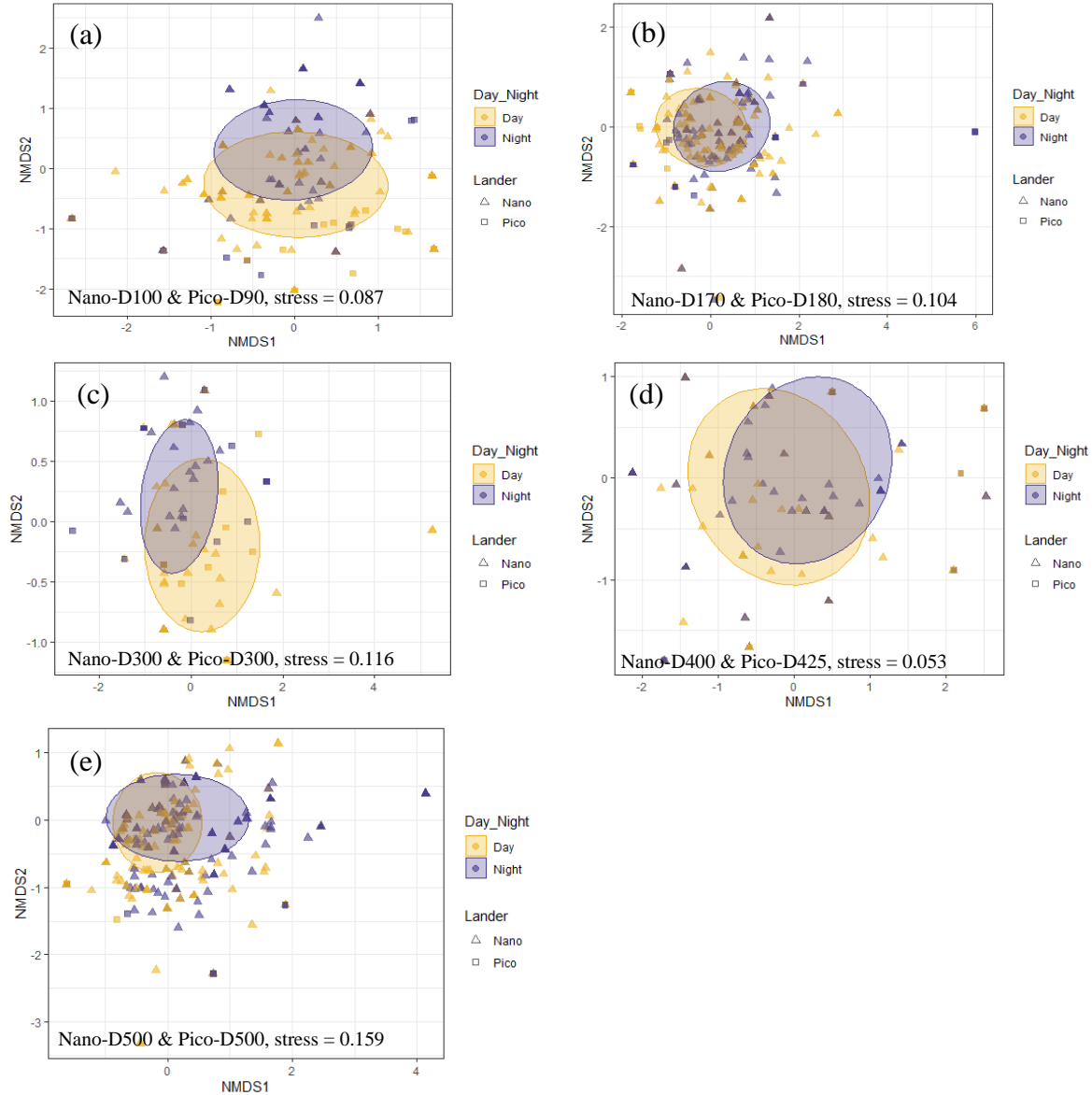
Figure 14: nMDS plots of depths colored to show the effects of day versus night on the community. All deployments were conducted using the Nanolander and the Picolander in the La Jolla Canyon and only Nanolander samples with A or A- visibility were used in these analyses. Yellow points represent sample during the day while the blue points represent samples during the night. Ellipses represent grouping category and 50% confidence limits.
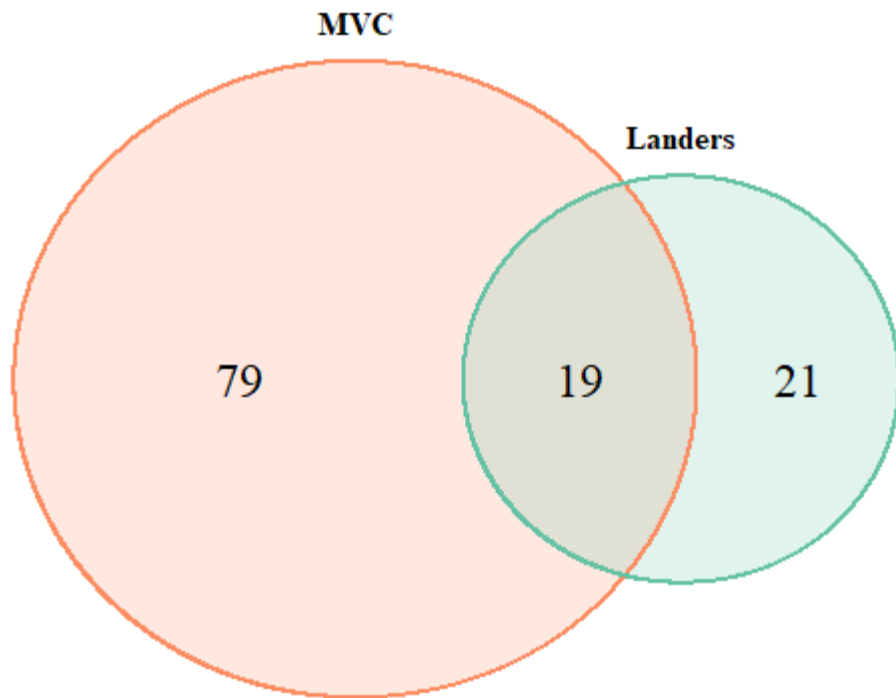
Figure 15: A Venn diagram displaying the number of La Jolla Canyon specimens in the Marine Vertebrate Collection (MVC) at Scripps Institution of Oceanography (SIO) and the number of fish species observed by the landers in the La Jolla Canyon. The overlapping zone represents common species between the two methods.
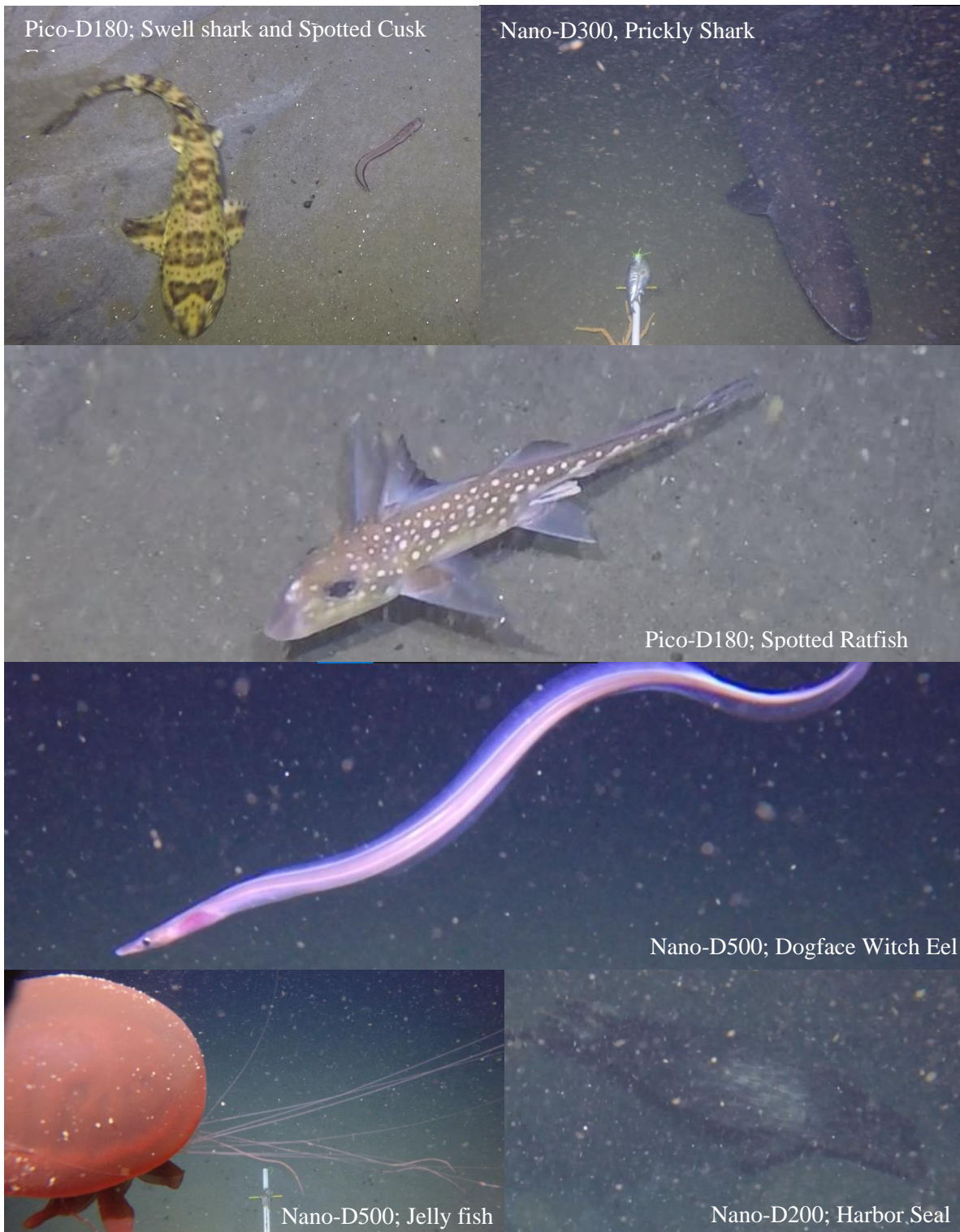
Figure 16: Images from various lander deployments to provide examples of image quality and unique species observed.
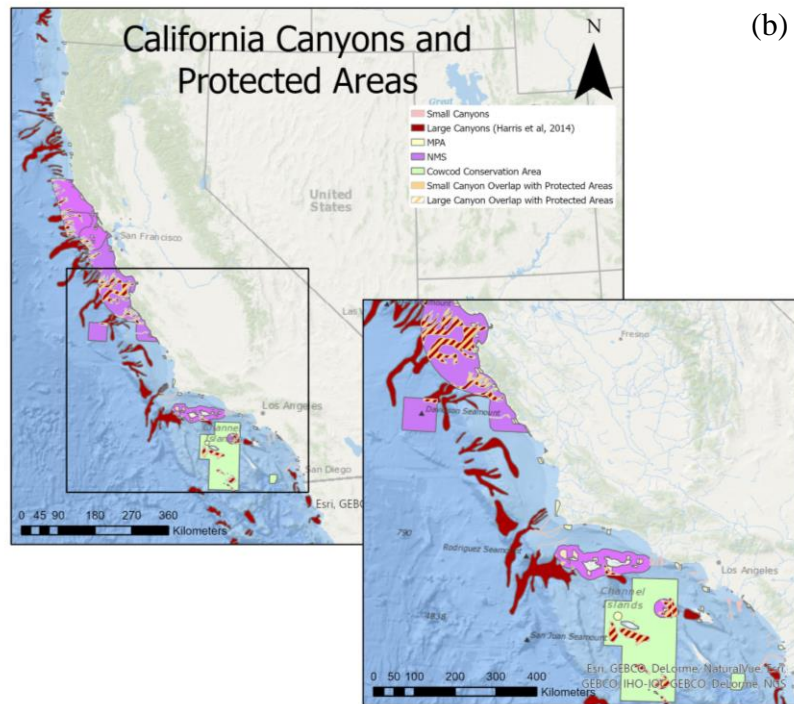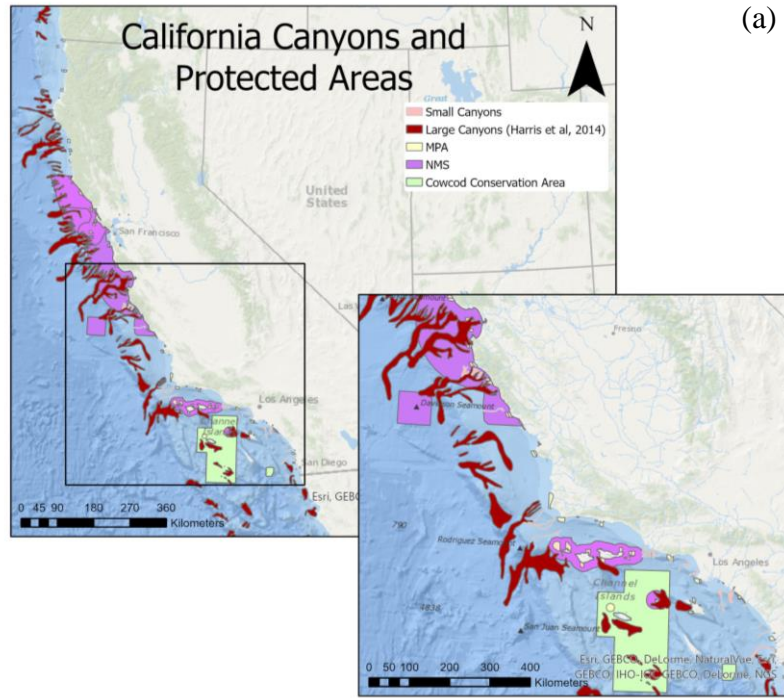
Figure 17: a) Map showing the large canyons (Harris et al, 2014) in red, small canyons in pink, and protected areas on the coast of California; b) Overlap between large canyons and protected areas is shown in hatched orange while small canyon and protected area overlap is shown in solid orange.

Supplementary Materials

Supplementary Table 1: Fish species observed in this study (Lander) or collected and archived in the Marine Vertebrate Collection, Scripps Institution of Oceanography (MVC) from the La Jolla Canyon. MVC data assembled in part from Hastings et al. (2014).

Family	Species	Common Name	Lander/Collection
Agonidae			
	Agonopsis sterletus	Spearnose Poacher	MVC
	Odontopyxis trispinosa	Pygmy Poacher	MVC
	Xeneretmus latifrons	Blacktip Poacher	MVC
	Xeneretmus ritteri	Stripefin Poacher	Lander
Anarhichadidae			
	Anarrhichthys ocellatus	Wolf-eel	MVC
Anoplopomatidae			
	Anoplopoma fimbria	Sablefish	Lander; MVC
Bathylagidae			
	Bathylagidae	Deep-sea Smelt	Lander
Bathymasteridae			
	Rathbunella alleni	Stripefin Ronquil	MVC
	Rathbunella hypoplecta	Bluebanded Ronquil	Lander, MVC
Batrachoididae			
	Porichthys notatus	Plainfin Midshipman	MVC
Bythitidae			
	Brosmophycis marginata	Red Brotula	MVC
Carangidae			
	Trachurus symmetricus	Jack Mackerel	MVC
Carcharhinidae			
	Prionace glauca	Blue Shark	MVC
Chimaeridae			
	Hydrolagus colliei	Spotted Ratfish	Lander; MVC
Cottidae			
	Chitonotus pugetensis	Roughback Sculpin	MVC
	Icelinus cavifrons	Pit-head Sculpin	MVC
	Icelinus filamentosus	Threadfin Sculpin	MVC
	Scorpaenichthys marmoratus	Cabezon	MVC

Cynoglossidae			
	Symphurus atricaudus	California Tonguefish	MVC
Echinorhinidae			
	Echinorhinus cookei	Prickly Shark	Lander
Embiotocidae			
	Phanerodon atripes	Sharpnose Seaperch	MVC
	Phanerodon vacca	Pile Perch	MVC
	Zalembius roseus	Pink Seaperch	MVC
Engraulidae			
	Engraulis mordax	Northern Anchovy	Lander
Etmopteridae			
	Centrocyllium nigrum	Combtooth Dogfish	Lander
Gobiidae			
	Rhinogobiops nicholsii	Blackeye Goby	MVC
Gonostomatidae			
	Cyclothone spp.	Bristlemouth	Lander
Heterodontidae			
	Heterodontus francisci	Horn Shark	MVC
Hexagrammidae			
	Hexagrammos decagrammus	Kelp Greenling	MVC
	Ophiodon elongatus	Lingcod	MVC
	Oxylebius pictus	Painted Greenling	MVC
Hexanchidae			
	Hexanchus griseus	Bluntnose Sixgill Shark	MVC
Labridae			
	Oxyjulis californica	Señorita	MVC
	Semicossyphus pulcher	California Sheephead	MVC
Lamnidae			
	Isurus oxyrinchus	Shortfin Mako	MVC
Latilidae			
	Caulolatilus princeps	Ocean Whitefish	Lander; MVC
Liparidae			
	Careproctus melanurus	Blacktail Snailfish	Lander, MVC
Macrouridae			
	Nezumia steligidolepis	California Grenadier	Lander
Merlucciidae			
	Merluccius productus	Pacific Hake	Lander; MVC

Myctophidae			
	Myctophidae	Latern Fish	Lander
Myliobatidae			
	Myliobatis californica	Bat Ray	MVC
Myxinidae			
	Eptatretus deanii	Black Hagfish	Lander
	Eptatretus mcconnaugheyi	Shorthead Hagfish	MVC
	Eptatretus stoutii	Pacific Hagfish	Lander; MVC
Nettastomatidae			
	Facciolella equatorialis	Dogface Witch Eel	Lander
Ophidiidae			
	Chilara taylori	Spotted Cusk-eel	Lander; MVC
	Ophidion scrippsae	Basketweave Cusk-eel	MVC
	Ophiodon elongatus	Lingcod	MVC
Opisthocentridae			
	Plectobranchus evides	Bluebarred Prickleback	MVC
Paralichthyidae			
	Citharichthys sordidus	Pacific Sanddab	MVC
	Citharichthys stigmaeus	Speckled Sanddab	MVC
	Citharichthys xanthostigma	Longfin Sanddab	MVC
	Hippoglossina stomata	Bigmouth Sole	MVC
	Paralichthys californicus	California Halibut	MVC
	Xystreurys liolepis	Fantail Sole	MVC
Pleuronectidae			
	Eopsetta jordani	Petrale Sole	MVC
	Glyptocephalus zachirus	Rex Sole	Lander
	Lepidopsetta bilineata	Rock Sole	MVC
	Lyopsetta exilis	Slender Sole	Lander
	Microstomus pacificus	Dover Sole	Lander
	Parophrys vetulus	English Sole	Lander; MVC
	Pleuronichthys coenosus	C-O Sole	MVC
	Pleuronichthys ritteri	Spotted Turbot	MVC
	Pleuronichthys verticalis	Hornyhead Turbot	MVC

Rajidae			
	Raja inornata	California Skate	MVC
	Raja rhina	Longnose Skate	MVC
	Raja stellulata	Starry Skate	MVC
Scombridae			
	Scomber japonicus	Pacific Chub Mackerel	MVC
Scorpaenidae			
	Scorpaena guttata	California Scorpionfish	MVC
Scyliorhinidae			
	Cephaloscyllium ventriosum	Swell Shark	Lander
Pentanchidae			
	Apristurus brunneus	Brown Catshark	Lander
Sebastidae			
	Sebastes alutus	Pacific Ocean Perch	MVC
	Sebastes auriculatus	Brown Rockfish	MVC
	Sebastes caurinus	Copper Rockfish	Lander; MVC
	Sebastes chlorostictus	Greenspotted Rockfish	MVC
	Sebastes constellatus	Starry Rockfish	Lander; MVC
	Sebastes dallii	Calico Rockfish	MVC
	Sebastes diploproa	Splitnose Rockfish	Lander; MVC
	Sebastes elongatus	Greenstriped Rockfish	MVC
	Sebastes ensifer	Swordspine Rockfish	MVC
	Sebastes entomelas	Widow Rockfish	MVC
	Sebastes eos	Pink Rockfish	MVC
	Sebastes flavidus	Yellowtail Rockfish	MVC
	Sebastes goodei	Chilipepper	MVC
	Sebastes hopkinsi	Squarespot Rockfish	MVC
	Sebastes lentiginosus	Freckled Rockfish	MVC
	Sebastes levis	Cowcod	MVC
	Sebastes melanostomus	Blackgill Rockfish	MVC
	Sebastes miniatus	Vermilion Rockfish	Lander; MVC
	Sebastes mystinus	Blue Rockfish	MVC
	Sebastes ovalis	Speckled Rockfish	MVC
	Sebastes paucispinis	Bocaccio	MVC
	Sebastes rosaceus	Rosy Rockfish	MVC
	Sebastes rosenblatti	Greenblotched Rockfish	MVC
	Sebastes ruberrimus	Yelloweye Rockfish	MVC
	Sebastes rubrivinctus	Flag Rockfish	Lander; MVC

	Sebastes saxicola	Stripetail Rockfish	MVC
	Sebastes semicinctus	Halfbanded Rockfish	Lander; MVC
	Sebastes serranoides	Olive Rockfish	Lander; MVC
	Sebastes serriceps	Treefish	MVC
	Sebastes simulator	Pinkrose Rockfish	MVC
	Sebastes umbrosus	Honeycomb Rockfish	MVC
	Sebastolobus alascanus	Shortspine Thornyhead	Lander; MVC
Serranidae			
	Paralabrax nebulifer	Barred Sand Bass	MVC
	Pronotogrammus multifasciatus	Threadfin Bass	MVC
Squalidae			
	Squalus suckleyi	Pacific Spiny Dogfish	MVC
Squantinidae			
	Squatina californica	Pacific Angel Shark	MVC
Sternoptychidae			
	Sternoptychidae	Hatchetfish	Lander
Synodontidae			
	Synodus lucioceps	California Lizard fish	Lander
Torpedinidae			
	Tetronarce californica	Pacific Electric Ray	MVC
	Torpedo californica	Pacific Torpedo Ray	Lander
Triakidae			
	Mustelus californicus	Gray Smoothhound	MVC
	Mustelus henlei	Brown Smoothhound	MVC
	Triakis semifasciata	Leopard Shark	MVC
Trichiuridae			
	Lepidopus fitchi	Pacific Scabbardfish	MVC
Zaniolepididae			
	Zaniolepis frenata	Shortspine Combfish	Lander; MVC
Zoarcidae			
	Lycodapus fierasfer	Blackmouth Eelpout	Lander
	Lycodes cortezianus	Bigfin Eelpout	Lander
	Lycodes diapterus	Black Eelpout	Lander
	Lycodes pacificus	Blackbelly Eelpout	Lander; MVC

Supplementary Figure 1: Figures of the landers described in the introduction on lander history. a) Ewing & Vine, 1938; b) Zobell, 1959; c) Isaacs, 1960; d) Moore, 1961; e) Snodgrass, 1968; f) Phleger & Soutar, 1971; g) Priede & Bagely, 2000; h) Jamieson, 2009; i) Peoples et al., 2019; j) T. Miwa, 2016.

69

References

Berger, W. H., & Parker, F. L. (1970). Diversity of Planktonic Foraminifera in Deep-Sea Sediments. Science, 168(3937), 1345. https://doi.org/10.1126/science.168.3937.1345

Black, K. S., Fones, G. R., Peppe, O. C., Kennedy, H. A., & Bentaleb, I. (2001). An autonomous benthic lander:: preliminary observations from the UK BENBO thematic programme. Continental Shelf Research, 21(8), 859-877. https://doi.org/https://doi.org/10.1016/S0278-4343(00)00116-3

Brueggeman, P. (2009). La Jolla Canyon and Scripps Canyon Bibliography. https://doi.org/10.13140/RG.2.2.13623.16806

California. Department of Fish and Game. Marine Resources Region. (2003). California Cowcod Conservation Areas, 2003. [Shapefile]. Retrieved from https://earthworks.stanford.edu/catalog/stanford-kv299cy7357

C. De Leo, F., & Puig, P. (2018). Bridging the gap between the shallow and deep oceans: The key role of submarine canyons. Progress in Oceanography, 169, 1-5. https://doi.org/https://doi.org/10.1016/j.pocean.2018.08.006

Company, J. B., Maiorano, P., Tselepides, A., Politou, C. Y., Plaity, W., Rotllant, G., & Sardá, F. (2004). Deep-sea decapod crustaceans in the western and central Mediterranean Sea: preliminary aspects of species distribution, biomass and population structure. Scientia Marina, 68(S3), 73-86. https://doi.org/10.3989/scimar.2004.68s373

De Leo, F., Vetter, E., Smith, C., Rowden, A., & McGranaghan, M. (2014). Spatial scale-dependent habitat heterogeneity influences submarine canyon macrofaunal abundance and diversity off the Main and Northwest Hawaiian Islands. Deep Sea Research Part II: Topical Studies in Oceanography, 104, 267–290. https://doi.org/10.1016/j.dsr2.2013.06.015

De Leo, F. C. (2012). Submarine canyons: Hotspots of deep-sea benthic abundance and biodiversity (Publication Number 3534565) [Ph.D., University of Hawai'i at Manoa]. Earth, Atmospheric & Aquatic Science Collection; ProQuest Dissertations & Theses A&I. Ann Arbor. https://search.proquest.com/docview/1267132329?accountid=14524http://ucelinks.cdlib.org:8888/sfx_local?url_ver=Z39.88-2004&rft_val_fmt=info:ofi/fmt:kev:mtx:dissertation&genre=dissertations+%26+theses&sid=ProQ:ProQuest+Dissertations+%26+Theses+A%26I&atitle=&title=Submarine+canyons%3A+Hotspots+of+deep-sea+benthic+abundance+and+biodiversity&issn=&date=2012-01-01&volume=&issue=&spage=&au=De+Leo%2C+Fabio+Cabrera&isbn=978-1-267-81742-6&jtitle=&btitle=&rft_id=info:eric/&rft_id=info:doi/

Fernandez-Arcaya, U., Ramirez-Llodra, E., Aguzzi, J., Allcock, A. L., Davies, J. S., Dissanayake, A., Harris, P., Howell, K., Huvenne, V. A. I., Macmillan-Lawler, M., Martín, J., Menot, L., Nizinski, M., Puig, P., Rowden, A. A., Sanchez, F., & Van den Beld, I. M. J. (2017a). Ecological Role of Submarine Canyons and Need for Canyon Conservation: A Review [Review]. Frontiers in Marine Science, 4(5). https://doi.org/10.3389/fmars.2017.00005

Fernandez-Arcaya, U., Ramirez-Llodra, E., Aguzzi, J., Allcock, A. L., Davies, J. S., Dissanayake, A., . . . Van den Beld, I. M. J. (2017). Ecological Role of Submarine Canyons and Need for Canyon Conservation: A Review [Review]. *Frontiers in Marine Science*, *4*(5). https://doi.org/10.3389/fmars.2017.00005

Gallo, N. D. (2018). *Influence of ocean deoxygenation on demersal fish communities: Lessons from upwelling margins and oxygen minimum zones* (Doctoral dissertation). *UC San Diego*. ProQuest ID: Gallo_ucsd_0033D_17925. Merritt ID: ark:/13030/m5ff8qk7. Retrieved from https://escholarship.org/uc/item/6bb6v4z8

Gallo, N. D., Hardy, K., Wegner, N. C., Nicoll, A., Yang, H., & Levin, L. A. (2020). Characterizing deepwater oxygen variability and seafloor community responses using a novel autonomous lander. Biogeosciences, 17(14), 3943-3960. https://doi.org/10.5194/bg-17-3943-2020

Hamann, M. (2019). *The dynamics of internal tides and mixing in coastal systems* (Doctoral dissertation). *UC San Diego*

Harris, P., & Whiteway, T. (2011). Global distribution of large submarine canyons: Geomorphic differences between active and passive continental margins. Marine Geology, 285, 69-86. https://doi.org/10.1016/j.margeo.2011.05.008

Hastings, P., Craig, M., Erisman, B., Hyde, J., & Walker, H. (2014). Fishes of Marine Protected Areas Near La Jolla, California. Bulletin, Southern California Academy of Sciences, 113, 200-231. https://doi.org/10.3160/0038-3872-113.3.200

Heck Jr, K. L., van Belle, G., & Simberloff, D. (1975). Explicit Calculation of the Rarefaction Diversity Measurement and the Determination of Sufficient Sample Size [https://doi.org/10.2307/1934716]. Ecology, 56(6), 1459-1461. https://doi.org/https://doi.org/10.2307/1934716

Huang, Z., Nichol, S. L., Harris, P. T., & Caley, M. J. (2014). Classification of submarine canyons of the Australian continental margin. Marine Geology, 357, 362-383. https://doi.org/https://doi.org/10.1016/j.margeo.2014.07.007

Hurlbert, S. H. (1971). The Nonconcept of Species Diversity: A Critique and Alternative Parameters [https://doi.org/10.2307/1934145]. Ecology, 52(4), 577-586. https://doi.org/https://doi.org/10.2307/1934145

Inman, D. L. (2005). Littoral Cells. In M. L. Schwartz (Ed.), Encyclopedia of Coastal Science (pp. 594-599). Springer Netherlands. https://doi.org/10.1007/1-4020-3880-1_196

Isaacs, J. D., & Schick, G. B. (1960). Deep-sea free instrument vehicle. Deep Sea Research (1953), 7(1), 61-67. https://doi.org/https://doi.org/10.1016/0146-6313(60)90009-5

Jahnke, R. A., & Christiansen, M. B. (1989). A free-vehicle benthic chamber instrument for sea floor studies. Deep Sea Research Part A. Oceanographic Research Papers, 36(4), 625-637. https://doi.org/https://doi.org/10.1016/0198-0149(89)90011-3

Jamieson, A., Solan, M., & Fujii, T. (2009). Imaging Deep-Sea Life Beyond the Abyssal Zone. Sea Technology, 50, 41-46.

Jobstvogt, N., Townsend, M., Witte, U., & Hanley, N. (2014). How Can We Identify and Communicate the Ecological Value of Deep-Sea Ecosystem Services? *PloS one*, *9*, e100646. https://doi.org/10.1371/journal.pone.0100646

Kunze, E., Rosenfeld, L. K., Carter, G. S., & Gregg, M. C. (2002). Internal Waves in Monterey Submarine Canyon. Journal of Physical Oceanography, 32(6), 1890-1913. https://doi.org/10.1175/1520-0485(2002)032<1890:iwimsc>2.0.co;2

Levin, L. A., Bett, B. J., Gates, A. R., Heimbach, P., Howe, B. M., Janssen, F., McCurdy, A., Ruhl, H. A., Snelgrove, P., Stocks, K. I., Bailey, D., Baumann-Pickering, S., Beaverson, C., Benfield, M. C., Booth, D. J., Carreiro-Silva, M., Colaço, A., Eblé, M. C., Fowler, A. M., Gjerde, K. M., Jones, D. O. B., Katsumata, K., Kelley, D., Le Bris, N., Leonardi, A. P., Lejzerowicz, F., Macreadie, P. I., McLean, D., Meitz, F., Morato, T., Netburn, A., Pawlowski, J., Smith, C. R., Sun, S., Uchida, H., Vardaro, M. F., Venkatesan, R., & Weller, R. A. (2019). Global Observing Needs in the Deep Ocean [Review]. Frontiers in Marine Science, 6(241). https://doi.org/10.3389/fmars.2019.00241

McClanahan, T. (2019). Coral reef fish communities, diversity, and their fisheries and biodiversity status in East Africa. Marine Ecology Progress Series, 632. https://doi.org/10.3354/meps13153

Miwa, T., Iino, Y., Tsuchiya, T., Matsuura, M., Takahashi, H., Katsuragawa, M., Fukuba, T., Furushima, Y., Fukuhara, T., Fukushima, T., & Yamamoto, H. (2016, 6-8 Oct. 2016). Underwater observatory lander for the seafloor ecosystem monitoring using a video system. 2016 Techno-Ocean (Techno-Ocean),

Moore, D. G. (1961). The free-corer; sediment sampling without wire and winch. Journal of Sedimentary Research, 31(4), 627-A-630. https://doi.org/10.1306/74d70c22-2b21-11d7-8648000102c1865d

Parker, W. R., Doyle, K., Parker, E. R., Kershaw, P. J., Malcolm, S. J., & Lomas, P. (2003). Benthic interface studies with landers. Consideration of lander/interface interactions and their design implications. Journal of Experimental Marine Biology and Ecology, 285-286, 179-190. https://doi.org/https://doi.org/10.1016/S0022-0981(02)00526-9

Peoples, L. M., Norenberg, M., Price, D., McGoldrick, M., Novotny, M., Bochdansky, A., & Bartlett, D. H. (2019). A full-ocean-depth rated modular lander and pressure-retaining sampler capable of collecting hadal-endemic microbes under in situ conditions. Deep Sea Research Part I: Oceanographic Research Papers, 143, 50-57. https://doi.org/https://doi.org/10.1016/j.dsr.2018.11.010

Phleger, C. F., & Soutar, A. (1971). Free Vehicles and Deep-Sea Biology. Integrative and Comparative Biology, 11, 409-418.

Priede, I. a. B. P. (2000). In situ studies on deep-sea demersal fishes using autonomous unmanned lander platforms. Oceanography and Marine Biology: an Annual Review, 38, 357-392.

Priede, I. G., Addison, S., Bradley, S., Bagley, P. M., Gray, P., Yau, C., Rolin, J., Blandin, J., Legrand, J., Cremer, A., Witte, U., Pfannkuche, O., Tengberg, A., Hulth, S., Helder, W., & Weering, T. V. (1998, 28 Sept.-1 Oct. 1998). Autonomous deep-ocean lander vehicles; modular approaches to design and operation. IEEE Oceanic Engineering Society. OCEANS'98. Conference Proceedings (Cat. No.98CH36259),

Sahoo, A., Dwivedy, S. K., & Robi, P. S. (2019). Advancements in the field of autonomous underwater vehicle. Ocean Engineering, 181, 145-160. https://doi.org/https://doi.org/10.1016/j.oceaneng.2019.04.011

Santora, J. A., Zeno, R., Dorman, J. G., & Sydeman, W. J. (2018). Submarine canyons represent an essential habitat network for krill hotspots in a Large Marine Ecosystem. Scientific Reports, 8(1), 7579. https://doi.org/10.1038/s41598-018-25742-9

Sayles, F. L., & Dickinson, W. H. (1991). The ROLAI2D lander: A benthic lander for the study of exchange across the sediment-water interface. Deep Sea Research Part A. Oceanographic Research Papers, 38(5), 505-529. https://doi.org/https://doi.org/10.1016/0198-0149(91)90061-J

Shanmugam, G. (2018). Slides, Slumps, Debris Flows, Turbidity Currents, and Bottom Currents: Implications☆. In Reference Module in Earth Systems and Environmental Sciences. Elsevier. https://doi.org/https://doi.org/10.1016/B978-0-12-409548-9.04380-3

Shantharam, A. K., Wei, C. L., Silva, M., & Baco, A. R. (2021). Macrofaunal diversity and community structure of the DeSoto Canyon and adjacent slope. Marine Ecology Progress Series, 664, 23-42.

Simberloff, D. (1972). Properties of the Rarefaction Diversity Measurement. The American Naturalist, 106(949), 414-418. https://doi.org/10.1086/282781

Snodgrass, F. E. (1968). Deep Sea Instrument Capsule. Science, 162(3849), 78. https://doi.org/10.1126/science.162.3849.78

Spagnoli, F., Penna, P., Giuliani, G., Masini, L., & Martinotti, V. (2019). The AMERIGO Lander and the Automatic Benthic Chamber (CBA): Two New Instruments to Measure Benthic Fluxes of Dissolved Chemical Species. Sensors, 19, 2632. https://doi.org/10.3390/s19112632

Tengberg, A., De Bovee, F., Hall, P., Berelson, W., Chadwick, D., Ciceri, G., Crassous, P., Devol, A., Emerson, S., Gage, J., Glud, R., Graziottini, F., Gundersen, J., Hammond, D., Helder, W., Hinga, K., Holby, O., Jahnke, R., Khripounoff, A., Lieberman, S., Nuppenau, V., Pfannkuche, O., Reimers, C., Rowe, G., Sahami, A., Sayles, F., Schurter, M., Smallman, D., Wehrli, B., & De Wilde, P. (1995). Benthic chamber and profiling landers in oceanography — A review of design, technical solutions and functioning. Progress in Oceanography, 35(3), 253-294. https://doi.org/https://doi.org/10.1016/0079-6611(95)00009-6